

Evolutionary Models for Type Ib/c Supernova Progenitors

Sung-Chul Yoon

Department of Physics and Astronomy, Seoul National University, Gwanak-ro 1, Gwanak-gu, Seoul, 151-742, Republic of Korea
 Email: yoons@astro.snu.ac.kr

(RECEIVED December 02, 2014; ACCEPTED March 24, 2015)

Abstract

SNe Ib/c mark the deaths of hydrogen-deficient massive stars. The evolutionary scenarios for SNe Ib/c progenitors involve many important physical processes including mass loss by winds and its metallicity dependence, stellar rotation, and binary interactions. This makes SNe Ib/c an excellent test bed for stellar evolution theory. We review the main results of evolutionary models for SN Ib/c progenitors available in the literature and their confrontation with recent observations. We argue that the nature of SN Ib/c progenitors can be significantly different for single and binary systems, and that binary evolution models can explain the ejecta masses derived from SN Ib/c light curves, the distribution of SN Ib/c sites in their host galaxies, and the optical magnitudes of the tentative progenitor candidate of iPTF13bvn. We emphasise the importance of early-time observations of light curves and spectra, accurate measurements of helium mass in SN Ib/c ejecta, and systematic studies about the metallicity dependence of SN Ib/c properties, to better constrain theories.

Keywords: binaries: general – stars: evolution – stars: massive – stars: Wolf–Rayet – supernovae: general

1 INTRODUCTION

Type I supernovae (SNe I) are characterised by the lack of prominent hydrogen lines in the spectra (e.g., Filippenko 1997). Strong helium lines are present in the spectra of SNe Ib, while they are practically absent in those of SNe Ic. SNe Ib/c are further distinguished from SNe Ia by the lack of strong Si II absorption line at 6355 Å. Most of ordinary SNe Ib/c, if not all, occur in star-forming galaxies, indicating that SNe Ib/c have a massive star origin (e.g., van den Berg, Li, & Filippenko 2005; Boissier & Prantzos 2009; Hakobyan et al. 2009; Kelly & Kirshner 2012; Anderson et al. 2012; Sander, Hamann, & Todt 2012). Their light curves are dominated by the energy release from radioactive ^{56}Ni as in the case of SNe Ia (Schaeffer, Casse, & Cahen 1987), but the inferred amounts of ^{56}Ni ejected by SNe Ib/c are similar, on average, to those of SNe II ($M^{56}\text{Ni} \sim 0.1 M_{\odot}$; e.g., Drout et al. 2011; Cano 2013; Lyman et al. 2014; Taddia et al. 2014) rather than SNe Ia ($M^{56}\text{Ni} \sim 1.0 M_{\odot}$; e.g., Stritzinger et al. 2006; Mazzali et al. 2007; Scalzo, Ruiter, & Sim 2014). The current consensus is that most of SNe Ib/c belong to a subset of core-collapse SNe that are SN explosions via collapse of the iron cores in massive stars at their deaths.

Hydrogen cannot be easily hidden in SN spectra (e.g., Elmhamdi et al. 2006; Spencer & Baron 2010; Dessart et al. 2011; Hachinger et al. 2012) and SN Ib/c progenitors must have lost their hydrogen envelopes by the time of explosion.

There exist mainly three possible ways for massive stars to become a hydrogen-deficient SN progenitor: mass loss from single stars via stellar winds (e.g., Chiosi & Maeder 1986), binary interactions (e.g., Podsiadlowski, Joss, & Hsu 1992), and chemically homogeneous evolution with rapid rotation (Maeder & Meynet 1987). The last mode of evolution have been invoked for explaining massive blue stragglers and long gamma-ray bursts (GRBs) within the collapsar scenario (Maeder 1987; Langer 1992; Yoon & Langer 2005; Woosley & Heger 2006; Yoon, Langer & Norman 2006; Yoon, Dierks, & Langer 2012a), but is not likely to be much relevant for the majority of SNe Ib/c that are found in the local Universe (Yoon et al. 2006).

In this review, we focus on ordinary SNe Ib/c: our objective here is to summarise theoretical results on SN Ib/c progenitors via single and binary evolutionary paths. We emphasise that each case has its own unique prediction that can be in principle well tested by observations. SNe Ib/c can therefore provide an invaluable insight on massive star evolution. Note that we restrict this review to the detailed properties of SNe Ib/c progenitors that are predicted by recent stellar evolution models. Progenitors of SN Iib (i.e., SNe of which the spectra have hydrogen lines at early times, but resemble those of SNe Ib at later times) are closely related to SN Ib/c progenitors, and will also be discussed briefly. Our discussions on observations, SN modelling, and stellar population studies will be highly biased by the selected topics we address

here. For more general topics on the evolution of massive stars and SN progenitors, readers are referred to the recent reviews by Maeder & Meynet (2000), Massey (2003), Heger et al. (2004), Smartt (2009), Langer (2012) and Smith (2014).

2 SINGLE STAR MODELS

2.1. Mass loss and final mass

It has been widely believed that Wolf–Rayet (WR) stars are observational counterparts of SNe Ib/c progenitors (e.g., Meynet & Maeder 2003; Massey 2003; Crowther 2007; Smartt 2009). Although helium stars as WR stars can be produced by binary interactions (e.g., Petrovic, Langer, & van der Hucht 2005a; Vanbeveren, Van Bever, & Belkus 2007), a large fraction of WR stars are found in isolation (van der Hucht 2001; Crowther 2007), and must have been produced from massive single stars¹ via mass loss due to stellar winds (the so-called Conti scenario; Conti 1976).

Evolutionary models of massive stars with mass loss predict that there exists an initial mass limit for WR stars, above which stars can lose the entire hydrogen envelope during the post-main-sequence phases (e.g., Maeder & Meynet 1987; Schaller et al. 1992; Vanbeveren, De Loore, & Van Rensbergen 1998; Meynet & Maeder 2003; Eldridge & Vink 2006; Georgy et al. 2012). A useful constraint on this mass limit can be provided by galactic WR stars. Observations indicate that WR stars of WN type in our Galaxy have the lower bolometric luminosity limit of $\log L/L_{\odot} \simeq 5.3$ (Hamann, Gräfenor, & Liermann 2006). This roughly corresponds to $10 M_{\odot}$ of a naked helium star, which requires an initial mass of about $25 M_{\odot}$. Stellar evolution models indicate that non-rotating stars at solar metallicity cannot lose their hydrogen envelope to become a WR star if $M_{\text{ZAMS}} < 40 M_{\odot}$, with the most commonly adopted mass-loss rate from red supergiant stars given by de Jager, Nieuwenhuijzen, & van der Hucht (1988). Enhancement of mass loss due to rotation or pulsation compared to the de Jager rate and some alternative empirical mass-loss prescriptions have been invoked to resolve this discrepancy (e.g., Vanbeveren et al. 1998; Salasnich, Bressan, & Chiosi 1999; Meynet & Maeder 2003; van Loon et al. 2005, 2008; Yoon & Cantiello 2010; Ekström et al. 2012).

Once a star becomes a WR star, further mass loss due to WR winds determines its final mass. In the 80s and 90s, a fixed value of about $3\text{--}8 \times 10^{-5} M_{\odot} \text{yr}^{-1}$ or mass-dependent values have been widely used for the WR mass-loss rate in most evolutionary models (Maeder & Meynet 1987; Langer 1989b; Schaller et al. 1992; Schaerer et al. 1993a, 1993b; Meynet et al. 1994; Woosley, Langer, & Weaver 1993, 1995). Later studies began to consider the WR mass-loss rate as a function of the luminosity and the surface abundances of helium and metals in a more explicit way (e.g., Well-

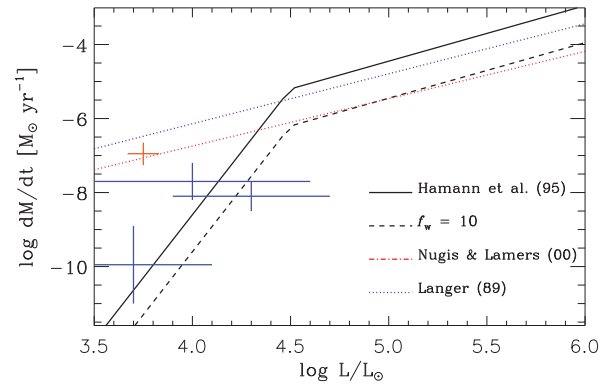


Figure 1. Comparison of different mass-loss prescriptions of massive helium stars on the zero-age helium main sequence as a function of the surface luminosity, which are based on WR stars ($\log L/L_{\odot} > 4.5$). The dot-dashed line and the dotted line give the WR mass-loss rates by Nugis & Lamers (2000) and Langer (1989b), respectively. The solid line denotes the mass-loss rate prescription given by Equation (1): the WR mass-loss rate by Hamann, Koesterke, & Wessolowski (1995) for $\log L/L_{\odot} \geq 4.5$ and the mass-loss rate of relatively low-mass helium stars for $\log L/L_{\odot} < 4.5$, which is based on the extreme helium stars analysed by Hamann, Schoenberner, & Heber (1982). The blue data points with the error bars are the mass-loss rates of these extreme helium stars. The orange point with the error bars denotes the mass-loss rate of the quasi-WR star HD 45166 (van Blerkom 1978; Groh, Oliveira, & Steiner 2008). The dashed line is 10 times lower than the solid line: f_w is the reduction factor compared to the mass-loss rate given by Equation (1).

stein & Langer 1999; Meynet & Maeder 2003, 2005; Eldridge & Vink 2006; Georgy et al. 2012). More important, with the growing evidence for hydrodynamic clumping of WR wind material, recent estimates for the WR mass-loss rate give significantly lower values than previously thought (e.g., see Figure 1; Nugis & Lamers 2000; Hamann et al. 2006; Crowther 2007; Sander et al. 2012). Several different prescriptions for the WR mass-loss rate are compared in Figure 1.

The single star models produced later than 2 000 predict systematically higher final masses of SN Ib/c progenitors than those in the 80s and 90s, as summarised in Figure 2. For example, with Langer’s mass-dependent WR mass-loss rate (Langer 1989b), a $60 M_{\odot}$ star at solar metallicity can become an SN Ib/c progenitor with an final mass as low as $4.25 M_{\odot}$ (Woosley et al. 1993). By contrast the models with the WR mass-loss rate of Nugis & Lamers (2000) give final masses higher than $10 M_{\odot}$, at solar metallicity.

This high final mass ($M_f > 10 M_{\odot}$) has consequences on the SN explosion. First of all, such massive helium stars have large amounts of binding energy. This would make successful explosion of these progenitors difficult: they may collapse to a black hole, without making an ordinary SN Ib/c (e.g., Heger et al. 2004, and references therein). Secondly, even if they exploded successfully, the resultant light curves would be too broad to be compatible with observations (Woosley et al. 1993, 1995; Dessart et al. 2011; Drout et al. 2011; Cano 2013; Lyman et al. 2014; Taddia et al. 2014). This brings into question the importance of single WR stars as progenitors of

¹ Some massive single stars on the main sequence may be products of binary mergers, but here we do not distinguish them from singly-formed massive stars.

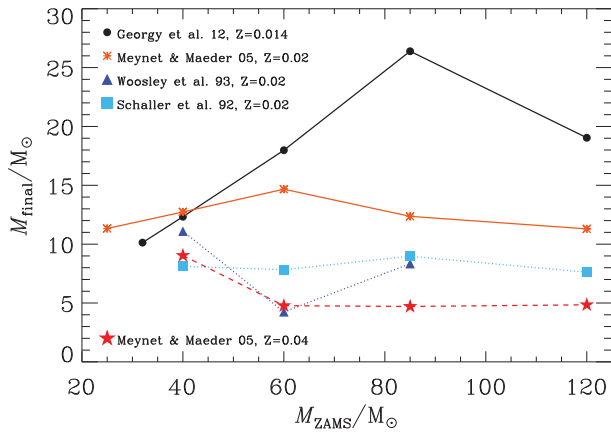


Figure 2. Theoretical predictions on the final mass of single star progenitors for SNe Ib/c, as a function of the initial mass (i.e., mass on the zero-age main sequence). Circle: rotating models of Georgy et al. (2012) at $Z = 0.014$, Asterisk: rotating models of Meynet & Maeder (2003) at $Z = 0.02$, Star: rotating models of Meynet & Maeder (2005) at $Z = 0.04$ with a metallicity-dependent WR mass-loss rate. Triangle: non-rotating models of Woosley et al. (1993) at $Z = 0.02$, Square: non-rotating models of Schaller et al. (1992) at $Z = 0.02$.

SNe Ib/c at solar metallicity. However, the role of single stars at super-solar metallicity may be significant given their relatively low final masses (Figure 2).

2.2. Surface properties

WR stars have large convective cores, being close to the Eddington limit, and rapidly lose the outer helium-rich layers by WR winds. This makes them almost chemically homogeneous. Therefore, stellar evolution models predict that WR stars evolve systematically bluewards on the HR diagram (e.g., Georgy et al. 2012; Yoon et al. 2012b; Eldridge et al. 2013), in contrast to the case of the evolution of hydrogen-rich stars which evolve redwards in general. The surface composition of chemical elements also evolves. First, as the residual of the hydrogen envelope is removed by winds, they evolve from WNL type to WN type. As they lose more mass, the products of helium burning including carbon and oxygen begin to appear at the surface, to become WC and WO stars (Figure 3). The general consensus is that WR stars from sufficiently high initial masses evolve according to the following order: WNL \rightarrow WN \rightarrow WC \rightarrow WO.²

In this scenario, WR stars should become more compact as they evolve from WNL to WO. Indeed, WNL and WO stars in our galaxy have lowest and highest surface temperatures, respectively, in agreement with the theoretical prediction (Hamann et al. 2006; Sander et al. 2012). But stellar

²WNL: Late type WR stars having strong emission lines from ionized nitrogen, which usually have a substantial amount of hydrogen.

WN, WC and WO: Early type WR stars for which emission lines from ionized nitrogen, carbon and oxygen are dominantly seen in the spectra, respectively.

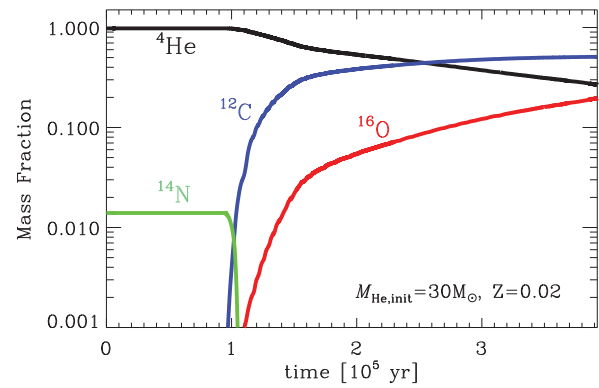


Figure 3. Evolution of the chemical composition at the surface of a $30\text{-}M_{\odot}$ helium star at $Z = 0.02$, with the WR mass-loss rate by Nugis & Lamers (2000). The calculation was terminated at the end of core neon burning.

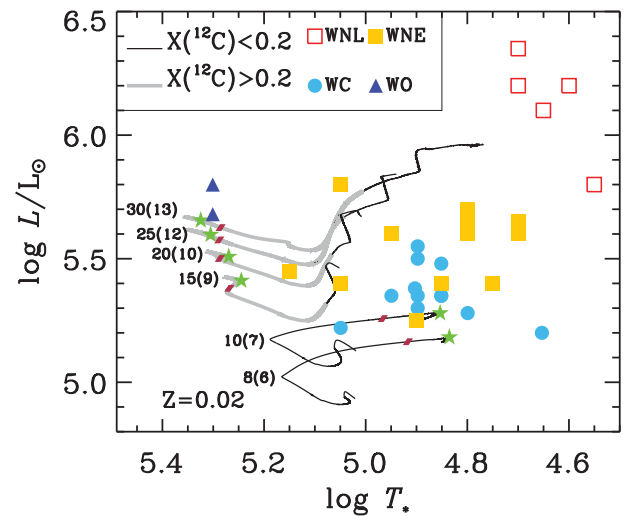


Figure 4. Evolution of massive helium stars at solar metallicity compared to the observed Wolf-Rayet stars in our galaxy on the Hertzsprung–Russell diagram. The WR mass-loss rate prescription by Nugis & Lamers (2000) was adopted in the evolutionary models. The initial mass for each evolutionary track is marked by the label in the left-hand side, and the final mass is indicated in the parenthesis. The thick grey lines mark the evolutionary stage where the surface mass-fraction of carbon is higher than 0.2. The star symbol denotes the end point of the evolution, which is the end of core neon burning. This figure is a reproduction of Figure 3 in Yoon et al. (2012b) with permission from Astronomy & Astrophysics, © ESO.

evolution models have great difficulty in explaining many of the surface properties of WR stars. In particular, the observed WR stars are found to have much larger radii and lower surface temperatures than what the evolutionary models predict (e.g., Hamann et al. 2006; Crowther 2007; Sander et al. 2012). The reason for this discrepancy is not well understood yet. Inflation of the envelope with a density inversion is observed in WR star models near the Eddington limit in hydrostatic equilibrium (Ishii, Ueno, & Kato 1999; Petrovic, Pols, & Langer 2006), but this is still not sufficient to fit observations as seen in Figure 4. A recent suggestion is that

the observationally implied inflation of WR stars may result from density inhomogeneities and the consequent enhancement of opacity in the sub-surface convective layer (Gräfener, Owocki, & Vink 2012).

This envelope inflation affects the bolometric correction, making WR stars fairly luminous in the optical ($M_V \lesssim -4$). If the optical luminosities of the observed WR stars represented those of SN Ib/c progenitors at the pre-SN stage, the previous search for an SN Ib/c progenitor in pre-SN images would have been successful (Maund & Smartt 2005; Maund, Smartt, & Schweizer 2005; Crockett et al. 2007; Smartt 2009; Eldridge et al. 2013). As of today, only one tentative identification has been reported with the SN Ib iPTF13bvn (Cao et al. 2013). All of the other searches for SN Ib/c progenitors have failed, even for the case with a very deep detection limit ($M_V \gtrsim -4.3$; Crockett et al. 2007; Eldridge et al. 2013). This result has often been interpreted as evidence for binary star progenitors (Crockett et al. 2007; Smartt 2009).

It should be noted that the majority of the observed WR stars must be on the helium main sequence, which is still far from the final evolutionary stage. After core helium exhaustion, the evolution of the core in a WR star is dominated by neutrino cooling and undergoes rapid Kelvin–Helmholtz contraction. With a sufficient amount of helium in the envelope, this would lead to further expansion of the helium envelope due to the so-called mirror effect. However, single WR stars would rapidly lose helium in the envelope as implied by the high mass-loss rate, and the overall radius would gradually decrease as the stellar evolution models predict. At the pre-SN stage, many WR stars would tend to become very hot, and optically faint like WO stars despite their very high bolometric luminosities (Yoon et al. 2012b). This means that the non-detection of most SN Ib/c progenitors in the previous attempts does not necessarily exclude single WR progenitors, and other constraints like ejecta masses of SNe Ib/c should also be taken into account to better understand the nature of SNe Ib/c progenitors.

2.3. Helium

The production of He I lines is found to depend both on the total He mass (Hachinger et al. 2012) and on the helium distribution in the envelope (Dessart et al. 2011, 2012a). Non-thermal excitation and ionisation of helium also play the key role for the formation of helium lines in SNe Ib (Lucy 1991; Woosley & Eastman 1997; Dessart et al. 2012a; Hachinger et al. 2012). This does not only require presence of helium in the progenitors, but also strong chemical mixing between helium in the envelope and radioactive ^{56}Ni produced in the innermost region of the SN ejecta (Dessart et al. 2012a; Hachinger et al. 2012). We still do not know exactly how much helium is needed for SNe Ib. This limit must depend on the degree of mixing of helium and nickel, which may in turn depend on the detailed structure of the progenitor and the energy and asymmetry of the explosion. Many authors

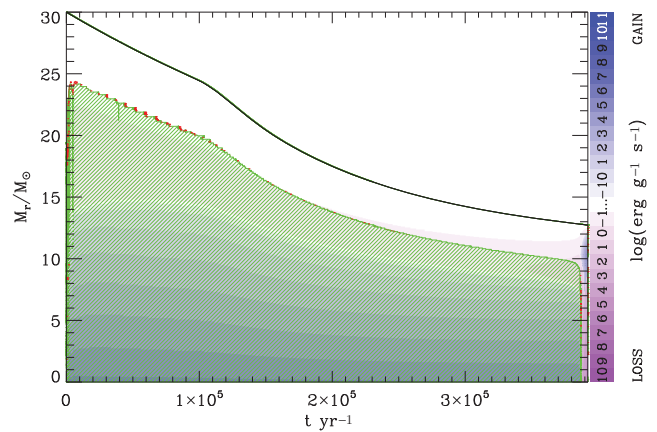


Figure 5. Evolution of the internal structure of a $30\text{-}M_{\odot}$ helium star, for which the Nugis and Lamers’ WR mass-loss rate was adopted. The helium-burning convective core is marked by the hatched lines. The black solid line marks the surface of the star. The calculation was terminated at the end of core neon burning.

simply assume a certain amount of helium (e.g., $0.5\text{--}0.6\text{ }M_{\odot}$) as the lower limit for SN Ib progenitors (e.g., Wellstein & Langer 1999; Yoon, Woosley, & Langer 2010; Georgy et al. 2012). Recently, Hachinger et al. (2012) suggested $0.14\text{ }M_{\odot}$ as the maximum possible amount of helium that can be hidden in the SN spectra, based on a spectroscopic study of several SN Ib/c with relatively low inferred ejecta masses.

In the most recent single star models (Georgy et al. 2012), the total amounts of helium in SN Ib/c progenitors range from $0.28\text{ to }2.2\text{ }M_{\odot}$. This is significantly higher than the proposed limit of $0.14\text{ }M_{\odot}$ by Hachinger et al. In fact, helium mass as low as $0.14\text{ }M_{\odot}$ is very difficult to achieve with stellar evolution models. Woosley et al. (1993) found that a $60\text{-}M_{\odot}$ star can become a $4.25\text{-}M_{\odot}$ SN Ib/c progenitor with a WR mass-loss rate much higher than nowadays adopted, but even in this extreme case, the remaining helium mass was as large as $0.18\text{ }M_{\odot}$. The reason for this difficulty is largely related to the dynamical adjustment of the stellar structure of WR stars with mass loss. As shown in Figure 5 as an example, the size of the helium-burning convective core in a WR star decreases as the WR star loses mass by winds (Figure 5), and therefore some amount of helium can remain unburned until the end of core helium burning even if more than half of the initial mass is lost. The residual helium could be completely removed with efficient mass loss during the later evolutionary stages. The current models predict, however, that the effect of mass loss during the post helium burning phases is relatively minor mainly because of the relatively short evolutionary time. We discuss the problem of helium in SNe Ib/c progenitors in Section 3.4 in more detail.

The mass fraction of helium in the outermost layers can also play an important role for the early time light curves and spectra of SNe Ib/c. Dessart et al. (2011) showed that if the helium mass fraction is sufficiently large (~ 0.9), He I lines can be produced without the contribution of non-thermal

processes for several days after the shock breakout, while no helium lines are seen for a low helium mass fraction ($\lesssim 0.5$) even with a total helium mass of about $1 M_{\odot}$. Therefore, He I lines during the early epoch of an SN Ib/c will provide an important constraint on the progenitor. Recent single star models in the literature predict that helium mass fraction at the surface of SN Ib/c progenitors is below 0.4 except for a limited initial mass range above the critical mass for WR star progenitors (e.g., Meynet & Maeder 2003, 2005; Georgy et al. 2012), in contrast to the case of binary star models that predict the majority of SN Ib/c progenitors have a surface helium mass fraction higher than 0.9 (Section 3.4). Given that the total amount of helium is also systematically smaller in single star models than in binary star models as discussed below, this implies that single star evolution is probably prone to SNe Ic.

2.4. Rotation

Super-luminous supernovae (SLSNe) and very energetic explosions like GRBs can be driven by rapid rotation. The most commonly invoked mechanisms for these events include the collapsar scenario (Woosley et al. 1993; MacFadyen & Woosley 1999) and the magnetar scenario (e.g., Wheeler et al. 2000; Burrows et al. 2007; Kasen & Bildsten 2010; Woosley 2010). So far, all of the supernovae associated with GRBs belong to Type Ic (Woosley & Heger 2006; Hjorth 2013), and many SLSNe are also found to be SNe Ic. While the collapsar scenario still remains most popular to explain GRBs (Woosley & Bloom 2006), the magnetar-driven explosion is nowadays the most invoked mechanism for the SLSNe Ic (e.g., Chomiuk et al. 2011; Dessart et al. 2012b; Inserra et al. 2013; Nicholl et al. 2013; Mazzali et al. 2014). The contending mechanism for SLSNe Ic is the pair-production instability (e.g., Barkat, Rakavy, & Sack 1967; Gal-Yam 2009; Kozyreva et al. 2014).

It is still a matter of debate which evolutionary channels of SNe Ib/c progenitors can lead to rotation-driven explosions like GRBs and SLSNe-Ic. Observations indicate that the majority of massive stars on the main sequence are rapid rotators, where the necessary condition for both collapsar and magnetar mechanism could be fulfilled if they retained the angular momentum until the pre-collapse stage (e.g., Heger, Langer, & Woosley 2000). However, massive stars may undergo angular momentum redistribution via mass loss due to stellar winds and/or binary interactions, and the transport of angular momentum (Maeder & Meynet 2000; Heger et al. 2000; Hirschi, Meynet, & Maeder 2004; Heger, Woosley, & Spruit 2005; Petrovic et al. 2005b; Yoon et al. 2010). The angular momentum transfer may occur on a dynamical timescale in convective layers by convection. In radiative layers, rotationally-induced hydrodynamic instabilities like the shear instability and Eddington–Sweet circulations may transport angular momentum (Maeder & Meynet 2000). Dynamo actions may also occur in radiative layers according to the so-called Tayler–Spruit dynamo theory (Spruit 2002),

which may cause strong magnetic torques across differentially rotating layers.

Theoretical studies indicate that, without magnetic fields, angular momentum transport is severely inhibited by the chemical stratification across the boundary between the stellar core and the hydrogen envelope (μ -barrier; Meynet & Maeder 1997; Heger et al. 2000). Single star progenitors of SNe Ib/c can thus retain a significant amount of angular momentum until the pre-SN stage, even though most of the initial angular momentum is lost by stellar winds (Heger et al. 2000; Hirschi et al. 2004); the predicted amounts of angular momentum in the cores are much more than what neutron stars can have at the break-up velocity, and enough to produce a long GRB within the collapsar scenario (Woosley 1993). This means that almost all SN Ib/c progenitors have enough angular momentum to form GRB/SLSN-Ic progenitors. Given that rapid rotation is only one necessary condition for collapsar/magnetar production, this should not necessarily lead to the conclusion that non-magnetic models predict too many GRBs and SLSNe-Ic compared to the observation. However, because such exotic explosions belong to a subset of SNe Ib/c, the result of non-magnetic models implies that GRBs and SLSNe-Ic should occur more frequently at higher metallicity as ordinary SNe Ib/c do, if mass loss by winds provided the main evolutionary path for their progenitors. Contrary to this expectation, observations indicate that low-metallicity is preferred for both GRBs and SLSNe-Ic (e.g., Modjaz et al. 2008; Graham & Fruchter 2013; Lunnan et al. 2014).

Magnetic torques can easily overcome the hindrance by the chemical stratification to the transport of angular momentum. Magnetic models with the Tayler–Spruit dynamo predict that single WR stars rotate too slowly to produce a magnetar/collapsar (Heger et al. 2005). This is consistent with the fact that GRBs and SLSNe-Ic are very rare. Magnetic models also better explain the spin rates of young millisecond pulsars.

Several authors have questioned the validity of the Tayler–Spruit dynamo theory (Zahn, Brun, & Mathis 2007; Gellert, Rüdiger, & Elstner 2008) and we still cannot draw any solid conclusion on which case between magnetic and non-magnetic models better represents the reality. However, it is not only massive stars but also intermediate- and low-mass stars that provide evidence for very efficient transport of angular momentum in the radiative layers. Such examples include slow rotation of isolated white dwarfs (Suijs et al. 2008), the radial velocity profile in the Sun (Eggenberger, Maeder, & Meynet 2005), and recent asteroseismic results of low-mass stars (Eggenberger, Montalbán, & Miglio 2012; Cantiello et al. 2014). Our tentative conclusion is that some strong braking mechanism like the Tayler–Spruit dynamo is actually working in stars, and that magnetic models may better explain recent observations in general. The role of magnetic fields on the evolution of stars still remains a very challenging subject of future study. Some other mechanisms like baroclinic instability (Fujimoto 1993) and pulsa-

tional instabilities (Townsend & MacDonald 2008) may also play an important role for the transport of angular momentum, but have not been extensively studied for massive stars yet.

3 BINARY STAR MODELS

3.1. Binary evolution towards an SN Ib/c

The majority of massive stars form in binary systems (e.g., see Sana et al. 2012, for a recent observational analysis on the population of binary systems). A large fraction of them are believed to experience binary interactions during the course of their evolution, mainly due to the increase of stellar radius. Once the more massive star (the primary star) fills the Roche lobe in a binary system, mass transfer to the less massive star (the secondary star) begins. Mass transfer can be unstable if the mass ratio of the stellar components (i.e., $q = M_2/M_1$ where M_1 and M_2 are the masses of the primary and secondary stars, respectively) is sufficiently small. Unstable mass transfer will lead the binary system to a contact phase, which may eventually make the stellar components merge to become a single star. Although binary mergers are related to many important topics like stellar rotation, peculiar SNe and long GRBs (Fryer & Heger 2005; de Mink et al. 2014; Justham, Podsiadlowski, & Vink 2014), here we focus our discussion on non-merging systems that can produce ordinary SNe Ib/c. Recent analyses also indicate that the fraction of stable binary systems is much higher than previously believed (Kobulnicky & Fryer 2007; Sana et al. 2012), and thus the event rate of SNe Ib/c can be well explained by binary progenitors (Kobulnicky & Fryer 2007; Smith et al. 2011).

In the literature, mass transfer is often categorised into Case A, Case B, and Case C, depending on the evolutionary stage of the primary star when it fills the Roche lobe (Kippenhahn & Weigert 1967; Lauterborn 1970), as the following:

- Case A mass transfer : mass transfer during the main sequence.
- Case B mass transfer : mass transfer during the helium core contraction phase.
- Case C mass transfer : mass transfer during the core helium burning and later evolutionary stages.

Some binary systems may undergo multiple mass transfer phases, depending on the initial orbital periods and masses of the stellar components. The mass transfer phases that follow Case A/B mass transfer are often denoted as the following:

- Case AB mass transfer : mass transfer from the primary star that has previously undergone the Case A mass transfer, during the helium core contraction phase.
- Case BB mass transfer : mass transfer from the primary star that has previously undergone Case B mass transfer,

during the late evolutionary stages (mostly after core helium exhaustion for SN Ib/c progenitors).

- Case ABB mass transfer : mass transfer from the primary star that has previously undergone Case AB mass transfer, during the late evolutionary stages (mostly after core helium exhaustion for SN Ib/c progenitors).

Helium stars as SN Ib/c progenitors can be made via Case B/AB mass transfer as illustrated in Figure 6. The initial mass of such a helium star corresponds to the helium core mass ($M_{\text{He-core}}$) of the primary star at the onset of Case B/AB mass transfer. For Case B systems, $M_{\text{He-core}}$ can be given by a well-defined function of the zero-age main sequence (ZAMS) mass of the primary star as shown in Figure 7.

The evolution of the helium stars produced via Case B/AB mass transfer largely depends on their masses. Stellar evolution models indicate that Case BB/ABB mass transfer occurs when the primary star becomes a helium giant if the helium star mass is initially less than about 3.5–4.0 M_{\odot} , depending on the adopted mass-loss rate and metallicity. More massive helium stars do not interact anymore with the secondary stars after Case B/AB mass transfer, but can still lose mass further by winds. WR winds may be induced if the helium star mass is sufficiently high ($\gtrsim 10 M_{\odot}$) but the mass-loss rate from less massive helium stars is not well constrained observationally because such relatively low-mass helium stars have been rarely observed (see Sections 3.3 and 3.9 below for more discussions).

It is not only the primary star, but also the secondary star that can produce an SN Ib/c. In a close binary system, the primary star will leave a compact star remnant if it explodes as an SN Ib/c via Case B/AB/BB/ABB mass transfer, or if it becomes a white dwarf via Case BB/ABB mass transfer (see Figure 6). Unless the binary system is unbound by a strong neutron star kick, it will form a common envelope after the core hydrogen exhaustion in the secondary star. A short-period binary system consisting of a helium star plus a compact star (white dwarf, neutron star, or black hole) will be produced after the common envelope ejection. Explosion of the helium star will then produce an SN Ib/c.

Note also that Figure 6 still does not depict all the possible binary paths for SNe Ib/c, and there may exist other relatively rare channels. For example, some authors found that with Case A mass transfer, the SN order can be reversed for a limited parameter space: the secondary star first explode as an SN Ib/c, followed by SN Ib/c explosion of the primary star as a helium star in isolation or in a compact binary system with a neutron star companion, depending on the impact of the neutron star kick (Pols 1994; Wellstein, Langer, & Braun 2001).

The contribution of each evolutionary path to the total production of SNe Ib/c may depend on several physical parameters. They include the so-called mass accretion efficiency (i.e., the ratio of the accreted mass onto the secondary star to the transferred mass from the primary star), the specific angular momentum of any matter that is not accreted on

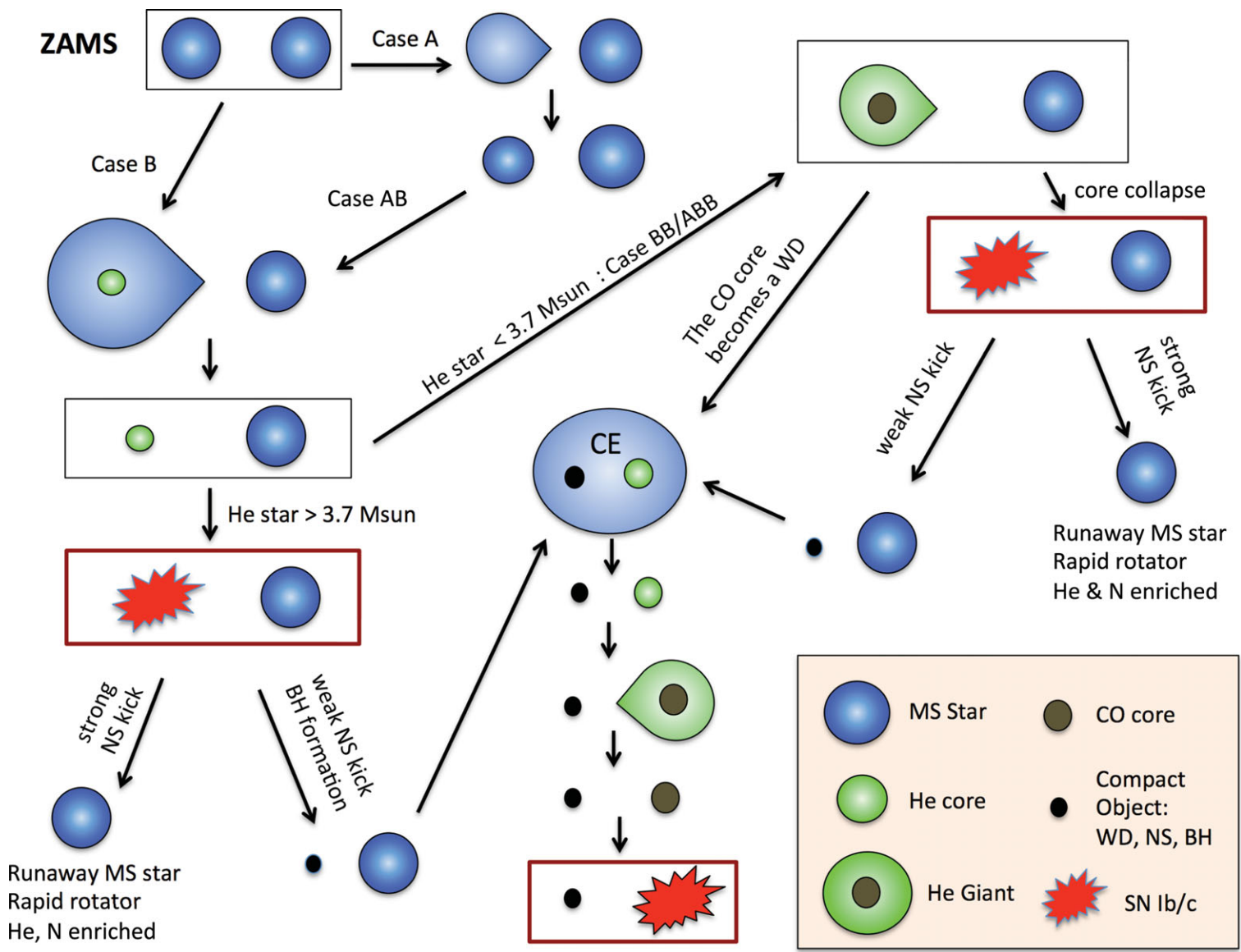


Figure 6. Evolutionary paths of a massive binary system towards a Type Ib/c supernova. The bifurcation points and the end points of the evolution are marked by square boxes.

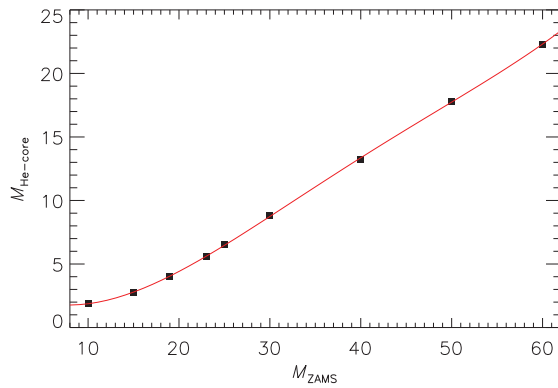


Figure 7. The helium core mass at the terminal age of the main sequence as a function of the initial mass for single stars. Based on non-rotating models without overshooting.

the secondary star but lost from the binary system, distribution of neutron star kick velocities, and the common envelope ejection efficiency (e.g., Podsiadlowski, Joss, & Hsu 1992). It is beyond the scope of this review to discuss all the details regarding binary population with respect to SNe Ib/c, and readers are referred to Podsiadlowski et al. (1992), Izzard, Ramirez-Ruiz, & Tout (2004), Eldridge, Izzard, & Tout (2008); Eldridge, Langer, & Tout (2011); Eldridge et al. (2013), as well as the contribution by de Mink in this issue. Here, it may be sufficient to say that the dominant channel to SNe Ib/c in binary systems is the Case B/BB, among others (Podsiadlowski et al. 1992). In the sections below, we focus on the detailed properties of SN Ib/c progenitors predicted from evolutionary models.

3.2. An example of binary models

To model the evolution of a binary system, we have to consider the change of the orbit due to stellar winds, mass transfer and/or gravitational wave radiation, and mass exchange between the stellar components via mass transfer. To investigate the effect of rotation, angular momentum exchange between stars and the orbit via tidal synchronisation and the spin-up effect of the secondary during the mass transfer phases should also be followed (see Langer 2012, for a recent review).

Many evolutionary models of massive binary stars have been presented in the literature, but only a limited number of studies aimed at detailed investigation of the structure of SNe Ib/c progenitors near/at the pre-SN stage (Woosley et al. 1995; Wellstein & Langer 1999; Yoon et al. 2010; Eldridge et al. 2013). Before we summarise the main results of these studies, we give an example for the evolution of relatively low-mass SN Ib/c progenitors, which is very different from that of massive WR stars.

The evolution of an SN Ib/c progenitor having $M_{ZAMS} = 16 M_{\odot}$ in a Case BB system is illustrated in Figures 8 and 9. After Case B mass transfer, the primary star becomes a hot and compact helium star. The surface hydrogen and helium mass fraction at this stage is about 0.28 and 0.7, respectively and a small amount of hydrogen of about $0.05 M_{\odot}$ is still retained in the outermost layer. As a result, the convective helium burning core can grow with hydrogen shell burning even though the total mass somewhat decreases due to mass loss by winds (Figure 9). This is contrasted to the case of mass-losing pure helium stars where the convective helium burning core shrinks in size in terms of the mass coordinate (Figure 5). During the post-helium burning stages, the he-

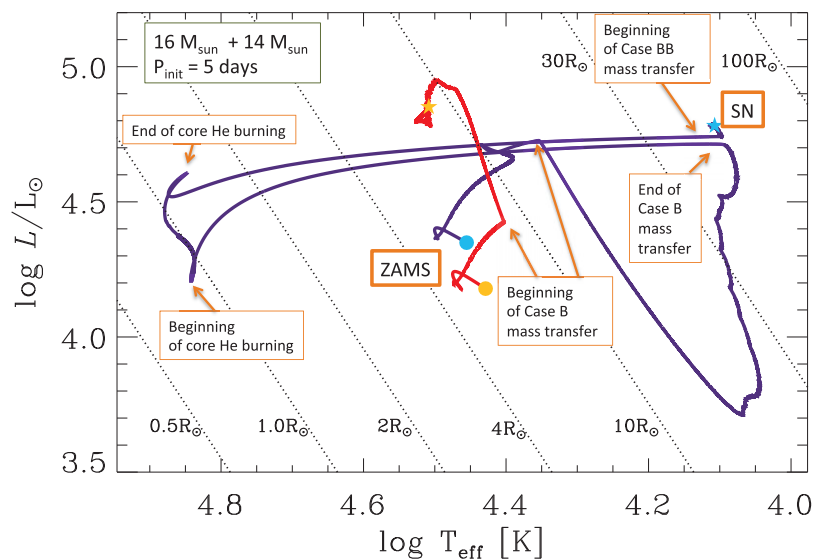


Figure 8. Evolution of a binary system consisting of $16 M_{\odot}$ plus $14 M_{\odot}$ stars with the initial period of 5 d. on the Hertzsprung–Russel diagram. The evolutionary tracks of the primary and secondary stars are marked by dark-blue and red colours, respectively. The adopted mass-loss rate for helium stars is given by Equation (1), reduced by a factor of 5 ($f_w = 5$). The initial and final points of each track are marked by the filled circle and the star symbol, respectively.

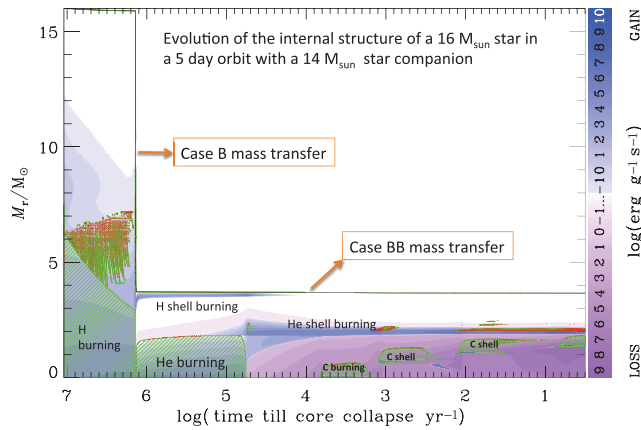


Figure 9. Evolution of the internal structure of the primary star in a binary system consisting of $16 M_{\odot}$ plus $14 M_{\odot}$ stars with the initial period of 5 d. Convective layers are marked by green hatched lines, and semi-convection layers by red dots. The surface of the star is indicated by the black solid line. The blue and pink colour shading marks net energy gain or loss from nuclear energy generation and neutrino emission.

lium envelope rapidly expands and Case BB mass transfer is initiated when carbon burning begins in the core (Figures 8 and 9). The SN explosion will occur when the surface temperature becomes fairly low ($\log T_{\text{eff}} \simeq 4.1$, Figure 8) while the star is still undergoing Case BB mass transfer. This is in stark contrast to the case of massive WR star progenitors that evolve bluewards throughout and explode when they become very hot ($\log T_{\text{eff}} > 5 \text{ K}$; Figure 4). The helium envelope expansion makes this binary progenitor bright in the optical bands compared to the case of WR progenitors, as discussed below (Section 3.7). Of course, more massive progenitors having $M_{\text{ZAMS}} \gtrsim 30$ will become a WR star even in binary systems after Case B/AB transfer, and evolve like a single WR star thereafter.

3.3. Mass loss and final mass

As mentioned above, one of the biggest uncertainties in the evolution of SN Ib/c progenitors is the mass-loss rate of naked helium stars. The mass-loss rate of WR stars ($\log L/L_{\odot} \gtrsim 5$) is relatively well known, but less luminous helium stars have not been well studied observationally. Several authors therefore used extrapolated values of the Nugis and Lamers rate or the Langer rate (see Figure 1) for the whole possible range of helium star mass (Woosley et al. 1995; Eldridge et al. 2008, 2013). On the other hand, Braun (1997) and Wellstein & Langer (1999) used a significantly reduced mass-loss rate for $\log L/L_{\odot} < 4.5$ as the following:

$$\log \left(\frac{\dot{M}}{M_{\odot} \text{yr}^{-1}} \right) = \begin{cases} -11.95 + 1.5 \log L/L_{\odot} & \text{for } \log L/L_{\odot} \geq 4.5 \\ -35.8 + 6.8 \log L/L_{\odot} & \text{for } \log L/L_{\odot} < 4.5. \end{cases} \quad (1)$$

Here the WR mass-loss rate for $\log L/L_{\odot} \geq 4.5$ is given by Hamann et al. (1995). The prescription for less luminous helium stars ($\log L/L_{\odot} < 4.5$) is based on the observations of extreme helium stars by Hamann et al. (1982). Figure 1 indicates that the simple extrapolation of the WR mass-loss rate down to $\log L/L_{\odot} < 4.5$ may lead to a significant overestimate even with the Nugis and Lamers rate, which is about 10 times lower than that of Hamann et al. (1995) for $\log L/L_{\odot} \geq 4.5$.

Given that the stellar wind mass-loss rates of massive stars were usually overestimated before the late-90s (see Section 2.1 above), mass-loss rates reduced by a certain factor (f_w) compared to that of Equation (1) were applied for some binary models of Wellstein & Langer (1999, $f_w = 2$) and for all the models of Yoon et al. (2010, $f_w = 5$ or 10). Note that the case of $f_w = 10$, for which the mass-loss rate becomes comparable to the Nugis and Lamers rate with $\log L/L_{\odot} \geq 4.5$, is still compatible with the observation of extreme helium stars of $\log L/L_{\odot} < 4.5$ (Figure 1). The caveat is that the extreme helium stars in the figure are giant stars at a pre-white dwarf stage, having masses of only about $0.8 M_{\odot}$ (Jeffery & Hamann 2010), and cannot represent ordinary SN Ib/c progenitors.

On the other hand, the quasi-WR (qWR) star HD 45166 is currently one of the most promising observational counterparts of relatively low-mass helium stars on the helium main sequence (Section 3.9). Its mass is about $4.2 M_{\odot}$ with a surface helium mass fraction of 0.5 and surface luminosity of $\log L/L_{\odot} = 3.75$. This star is likely on the helium main sequence. The estimated mass-loss rate gives a better agreement with the extrapolated value of the Nugis and Lamers rate than the mass-loss rates of extreme helium stars of Hamann et al. (1982). But we still have only one sample for such relatively low-mass helium stars in the core helium burning phase, and cannot make a solid conclusion on which mass-loss prescription is best suited for our purpose. As shown in Figure 10, however, this uncertainty does not make a great difference in terms of the final masses.

The predicted final masses of SN Ib/c progenitors that undergo Case B/BB mass transfer are given by Figure 10. The models in the figure, for which the considered initial period of the orbit ranges from 4 to 7 d, were taken from Wellstein & Langer (1999) and Yoon et al. (2010). In Wellstein & Langer (1999), conservative mass transfer (i.e., the mass accretion efficiency β , which is the ratio of the transferred matter from the primary to the accreted matter onto the secondary, equals to 1.0) was assumed and rotation was not taken into account. Yoon et al. (2010) considered the effects of rotation, with which β is self-regulated by the interplay between the mass transfer from the primary star and the mass-loss enhancement due to rotation from the secondary star that is spun-up by mass and angular momentum accretion. These models indicate $\beta \simeq 0.7$ for Case A mass transfer and $\beta = 0.0 \sim 0.8$ for Case B mass transfer, respectively.

For Case B systems, the final masses converge to about $3.15 M_{\odot}$ with $f_w = 1.0$ and gradually increases with

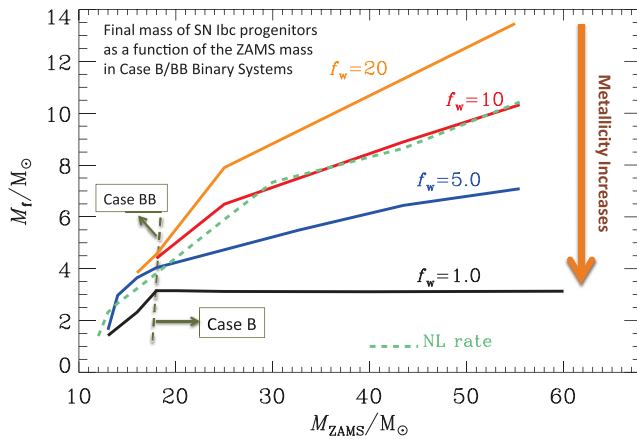


Figure 10. The final mass of SN Ib/c progenitors via Case B/BB mass transfer as a function of the initial mass, for different helium star mass-loss rates. Here f_w denotes the reduction factor that are applied to the mass-loss rate given by Equation (1): $f_w = 10$ and 20 roughly corresponds to solar and SMC metallicity, respectively. The presented results are based on the full binary models by Wellstein & Langer (1999) for $f_w = 1$ and the binary models and pure helium star models by Yoon et al. (2010) for the others. The boundary line between Case B and BB systems is marked by the dashed line. The data with $M_{ZAMS} \leq 25 M_\odot$ in Yoon et al. (2010) is based on the full binary evolution calculations but it is based on pure helium star models for $M_{ZAMS} > 25 M_\odot$ assuming that the pure helium star was produced via Case B mass transfer from the primary star with the corresponding ZAMS mass in a binary system. See Yoon et al. (2010) for more details. The result with the WR mass-loss rate by Nugis & Lamers (2000) at solar metallicity from unpublished binary star models (S.-C. Yoon, in preparation) is marked by the green dashed line, for which the boundary for Case B and BB shifts to about $M_{ZAMS} = 15 M_\odot$.

increasing M_{ZAMS} for $f_w = 5$ and 10 . The result with the Nugis and Lamers rate is comparable to that with $f_w = 10$. For $M_{ZAMS} \lesssim 18 M_\odot$, helium stars produced by Case B mass transfer undergoes Case BB mass transfer during carbon burning and later phases. Consequently the final masses for Case BB systems decrease more rapidly from this point with decreasing M_{ZAMS} , and the lower boundary of the ZAMS mass for SN Ib/c progenitors becomes about $12.5 M_\odot$, below which the primary star becomes a white dwarf.

In a Case A system, the primary star loses a significant fraction of the initial mass on the main sequence, and the helium core mass at the end of core hydrogen burning becomes lower than the corresponding Case B system. This makes the lower limit of ZAMS mass for SNe Ib/c shift to about $16 M_\odot$ for Case A systems (Wellstein & Langer 1999; Yoon et al. 2010). Very short orbits (typically $P_{\text{init}} < 5\text{d}$) are required for Case A systems, and their contribution to the SNe Ib/c rate from binary systems may be smaller by about a factor of 3–4 than that of Case B systems (cf. Sana et al. 2012).

These minimum ZAMS mass limits for SNe Ib/c (i.e., 12.5 and $16 M_\odot$ for Case B and Case A, respectively) are significantly higher than for SNe IIP from single stars, which is about 8 to $9 M_\odot$ (Smartt 2009; Ibeling & Heger 2013). Note that binary interactions can make this limit for SN IIP lowered even down to about $4 M_\odot$: for example, mergers of

$4 M_\odot$ plus $4 M_\odot$ star would make a $8 M_\odot$ SN IIP progenitor. Therefore, the stronger association of SNe Ib/c with younger stellar populations than SNe IIP in their host galaxies (e.g., Anderson et al. 2012; Kelly & Kirshner 2012; Sanders et al. 2012) is in qualitative agreement with the binary scenario.

According to the recent analyses of SN light curves (Drout et al. 2011; Cano 2013; Lyman et al. 2014; Taddia et al. 2014), SNe Ib/c have typically ejecta masses of 1 – $6 M_\odot$ ³. This means that, assuming the remnant mass of $1.4 M_\odot$, the final masses of ordinary SNe Ib/c range from 2.4 to $7.4 M_\odot$ at least. If some amounts of helium were hidden in these analyses as argued by Piro & Morozova (2014), the actual final mass would be somewhat higher. This observation is not compatible with the case of $f_w = 1$ in Figure 10, which predicts too low ejecta masses on average. The results with lower mass-loss rates give a better agreement: stars of $M_{ZAMS} = 14$ – $35 M_\odot$ can explain the observed ejecta mass range with $f_w = 10$ and the Nugis and Lamers rate for example. Lyman et al. (2014) also gives a similar conclusion from the comparison of their stellar population model with the observation.

The effect of different values of f_w can be regarded as the metallicity effect, because both observations and theories indicate that WR mass loss becomes stronger for higher metallicity (Vink & de Koter 2005; Crowther 2007; Gräfenr & Hamann 2008). The result in Figure 10 implies that SN Ib/c ejecta should be systematically more massive for lower metallicity, which can be tested by observations. If there were a certain mass cut for the boundary between successful SN explosion and black hole formation in terms of the final mass, this metallicity dependence of final masses would lead to gradual decrease of the SN Ib/c rate for decreasing metallicity (cf. Boissier & Prantzos 2009; Arcavi et al. 2010). For example, if $M_f = 8 M_\odot$ were the lower limit for BH formation, we would not expect an SN Ib/c explosion from $M_{ZAMS} \gtrsim 40 M_\odot$ at solar metallicity ($f_w \sim 10$) and $M_{ZAMS} \gtrsim 25 M_\odot$ at SMC metallicity ($f_w \sim 20$), respectively.

3.4. Helium

As discussed in Section 2.3, the amount of helium retained in progenitors may be one of the key factors that make the difference between SNe Ib and SNe Ic. As shown in Figure 11, helium mass varies from 0.1 to 1.9 for the considered range of ZAMS mass and mass-loss rates in Case B/BB systems. Helium mass (M_{He}) as a function of M_{ZAMS} has a local maximum at $M_\odot \sim 17$ to $18 M_\odot$ for $f_w = 1$ and 5 , and at $M_\odot \sim 30 M_\odot$ for $f_w = 20$, respectively. The rapid decrease of M_{He} as M_{ZAMS} approaches $12 M_\odot$ results from Case BB mass transfer, while the gradual decrease of M_{He} with increasing M_{ZAMS} is the effect of the increasing mass-loss rate.

³However, the systematic uncertainty on the inferred ejecta masses based on SNe Ib/c light curves can be large (up to a factor of 4 in principle) depending on the assumption for opacity and the method for measuring the light curve width (F. Bianco and M. Modjaz, private communication).

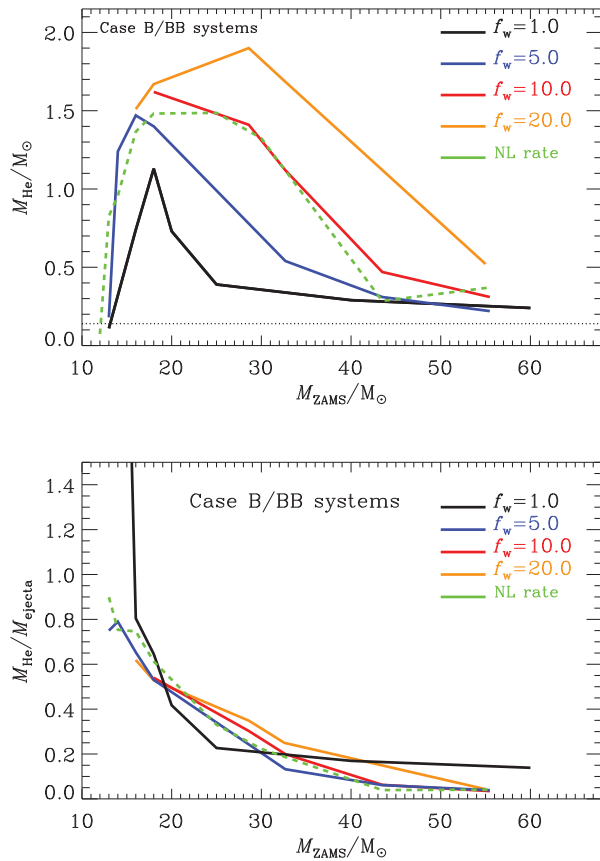


Figure 11. *Upper panel:* The total amounts of helium that are retained until the pre-SN stage in SN Ib/c progenitors via Case B/BB mass transfer, as a function of the initial mass for different loss rates of helium stars. Here f_w denotes the reduction factor that are applied to the mass-loss rate given by Equation (1) (see the figure caption of Figure 10). The NL rate means the WR mass-loss rate by Nugis & Lamers (2000). The data were taken from Wellstein & Langer (1999) for $f_w = 1$, Yoon et al. (2010) for $f_w = 5, 10$ and 20, and unpublished models by Yoon (in prep.) for the NL rate. *Lower panel:* The corresponding ratios of the helium to ejecta mass. Here we assumed that the remnant neutron star mass is $1.4 M_{\odot}$. See Figure 10 for the corresponding final mass.

It is important to note that, even for the case of very strong mass loss (i.e., $f_w = 1$), the amounts of helium at the pre-SN stage are significantly greater than the upper limit of $M_{\text{He}} = 0.14 M_{\odot}$ for SNe Ic that was suggested by Hachinger et al. (2012), except for the extreme Case BB case at around $M_{\text{ZAMS}} = 12.5\text{--}13.5 M_{\odot}$. Therefore, both single and binary star models cannot fulfil the condition of low amounts of helium for SN Ic. This might mean that, in reality, the chemical mixing between helium and nickel in SN ejecta is not as efficient as considered by Hachinger et al. (2012) for most SNe Ic (cf. Dessart et al. 2012a) such that more helium could be hidden. Such inefficient mixing is not usually supported by observations (e.g., Hachinger et al. 2012; Cano, Maeda, & Schulze 2014; Taddia et al. 2014)⁴, but we need a systematic

study on how the mixing efficiency via the Rayleigh–Taylor instability depends on the pre-SN structure of SNe Ib/c progenitors to resolve this issue.

Mass loss from helium stars is another uncertain factor that should be better understood. In particular, some helium stars can closely approach the Eddington limit during the final evolutionary stages if the mass is high enough. This might make the surface layers unstable to cause rapid mass eruption (cf., Maeder et al. 2012; Gräfener & Vink 2013), thus removing most of helium in the envelope shortly before the SN explosion as evidenced by many SNe Ib/c (Foley et al. 2007; Wellons, Soderberg, & Chevalier 2012; Gorbikov et al. 2014; Gal-Yam et al. 2014).

Eldridge et al. (2011) assumed a certain value of the ratio of the helium mass to the ejecta mass ($M_{\text{He}}/M_{\text{ejecta}}$) as the demarcation criterion between SN Ib and SN Ic. Because the chemical mixing between helium and nickel plays an important role for having helium lines in SN spectra, using $M_{\text{He}}/M_{\text{ejecta}}$ instead of M_{He} may be appropriate because a lower value of $M_{\text{He}}/M_{\text{ejecta}}$ means that helium can be more easily shielded from the gamma-ray photons produced in the innermost nickel-rich layer of the SN ejecta. Interestingly, Figure 11 indicates that $M_{\text{He}}/M_{\text{ejecta}}$ does not depend on the adopted mass-loss rate (hence on metallicity) as strongly as M_{He} does. This is because, for a lower mass-loss rate, the final mass and the CO core mass become higher and compensate the higher helium mass. This has important consequences in the prediction of SN Ib/c rate as a function of metallicity as discussed in Section 3.6 below.

If relatively low-mass helium star progenitors in binary systems have helium masses of about $1\text{--}1.5 M_{\odot}$ in their envelopes as the most recent models predict, this may lead to an early plateau phase due to helium recombination for several days as shown by Dessart et al. (2011). This prediction has recently been tentatively confirmed with the early-time light curve of SN Ib 2006lc (Taddia et al. 2014). Even in the absence of non-thermal effects, helium lines will also be observed during this phase, given that the mass fraction of helium in the envelope is very high (~ 0.98 ; see Section 2.3).

On the other hand, SN Ib/c progenitors with a compact star companion (see Figure 6) may undergo very strong mass transfer after core helium exhaustion, because these systems have a small mass ratio and short orbital period. Most of the helium envelope can be stripped off in this case, and very little helium will be left at the pre-SN stage (Pols & Dewi 2002; Dewi et al. 2002; Ivanova et al. 2003). This evolutionary channel has been often invoked to explain SNe Ic having low ejecta masses and fast declining light curves (e.g., Nomoto et al. 1994), including some ultra-faint SNe Ic (Tauris et al. 2013). The frequency of such events would be rare compared to ordinary SNe Ib/c, and its quantitative prediction heavily depends on the uncertain parameters related to the common envelope efficiency and neutron star kick.

⁴Liu et al. (2015, private communication) also show that the observed photospheric velocities and the equivalent widths of the O I 7774 line of SNe

Ib/c are not compatible with the predictions from progenitor models with a large amount of unmixed helium.

3.5. Hydrogen

Case B/AB mass transfer in a binary system stops when the hydrogen envelope of the primary star is almost stripped off, but it does not completely remove hydrogen. The amount of hydrogen remaining in the outermost layers of the helium core immediately after the mass transfer phase is typically $0.05\text{--}0.1 M_{\odot}$. Yoon et al. (2010) found that the final amount of hydrogen at the pre-SN stage is a function of the progenitor mass as the following. At solar metallicity, which roughly corresponds to the case with $f_w = 5 \dots 10$ in Figures 10 and 11 (see also Figure 1), no hydrogen will be left for helium stars having final masses of $M_f \gtrsim 4 \dots 4.4 M_{\odot}$. For the case of $M_f \lesssim 3 M_{\odot}$, Case BB/ABB mass transfer becomes efficient enough to completely remove hydrogen. For the final mass range in-between, the remaining hydrogen until SN explosion will be about $10^{-4} \dots 10^{-2} M_{\odot}$. On the other hand, the models with the Nugis and Lamers mass-loss rate at solar metallicity lose all the hydrogen in the envelope for the whole mass range (Eldridge et al. 2013; S.-C. Yoon, in preparation). Therefore, in principle, the signature of hydrogen in SN Ib/c progenitors can indirectly constrain the mass-loss rate from helium stars if we have good information about the metallicity in the vicinity of the SN site.

This small amount of hydrogen can be easily detected in the early time spectra of the resulting SN (Spencer & Baron 2010; Dessart et al. 2011), in which case it will be identified as an SN I Ib (cf. Chornock et al. 2011). These progenitors have relatively small radii ($R = 8 \dots 50 R_{\odot}$) compared to the yellow-supergiant SN I Ib progenitors (e.g., Maund et al. 2004; Van Dyk et al. 2014) produced via Case C mass transfer (Podsiadlowski et al. 1993; Claeys et al. 2011), and may belong to the compact category of SN I Ib (Chevalier & Soderberg 2010). Some authors argue that several SNe classified as Type Ib also have weak hydrogen absorption lines at high velocity (Deng et al. 2000; Branch et al. 2002; Elmhamdi et al. 2006). Therefore, whether the explosion of a helium star having a thin hydrogen layer may be recognised as SN I Ib or SN I c depends on the details of the SN observation.

The progenitor mass range for which a thin hydrogen layer is present at the pre-SN stage becomes widened and the total amount of remaining hydrogen increases with decreasing metallicity. The ratio of SN Ib/c to SN I Ib rate should decrease with decreasing metallicity (Figure 12).

3.6. Supernova types

From the above discussion, we can make a crude prediction on the SN types from Case B/BB mass systems as summarised in Figure 12. With Case AB/ABB systems, each boundary in the figure would simply shift to a higher M_{ZAMS} . For example, the lower limit of M_{ZAMS} for SN Ib/c from Case B/BB systems is about $12.5 M_{\odot}$, while it is about $16 M_{\odot}$ for Case AB/ABB systems. Because we still do not have any clear demarcation between SN Ib and SN Ic in terms of the progenitor structure (Section 3.4), ad hoc assumptions of

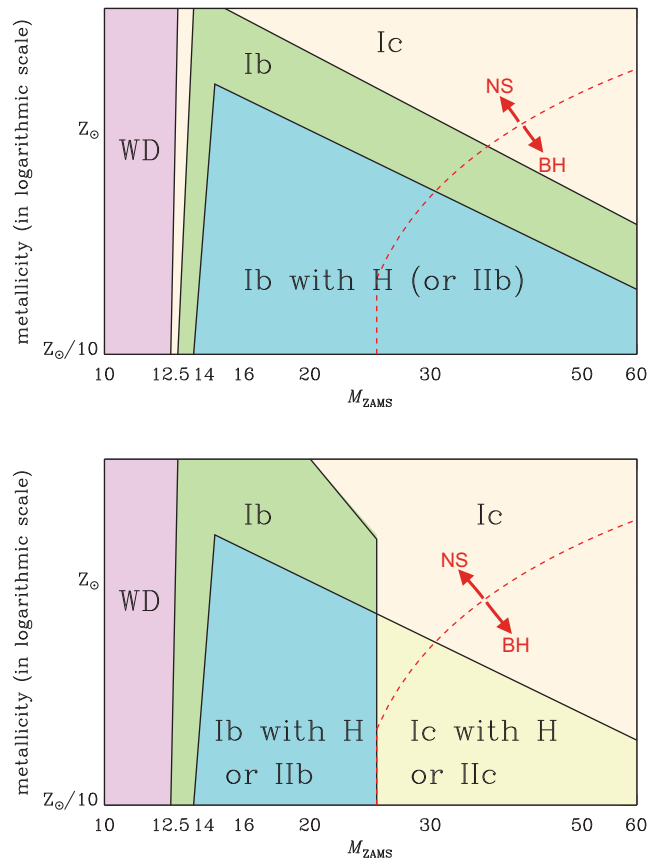


Figure 12. The predicted supernova types according to the initial mass and metallicity of primary stars in Case B/BB binary systems, based on the result presented in Figures 10 and 11. Here $M_{\text{He}} = 0.5$ and $M_{\text{He}}/M_{\text{ejecta}} = 0.45$ are adopted for the demarcation condition between SN Ib and SN Ic, for the upper (CASE I) and lower (CASE II) panels, respectively. The red dashed line denotes the critical limit for BH formation, assuming that $M_f > 8.0 M_{\odot}$ does not result in a neutron star (NS) remnant. Note that the figure provides only a qualitative prediction and the numbers that determine each boundary are subject to significant modification depending on the adopted assumptions.

$M_{\text{He}} = 0.5 M_{\odot}$ (CASE I) and $M_{\text{He}}/M_{\text{ejecta}} = 0.45$ (CASE II) were made for the upper and lower panels, respectively.

Several interesting predictions can be made from this figure, which should be tested in future observations. These predictions are only relevant for ordinary SNe Ib/c and those associated with GRBs or SLSNe-Ic are not considered here.

- For CASE I, the ratio of SN Ic to SN Ib rate from binary systems would decrease with decreasing metallicity in good agreement with Arcavi et al. (2010) and Modjaz et al. (2011), and SN Ic is hardly expected at sufficiently low metallicity. By contrast, this ratio would not necessarily decrease for decreasing metallicity with CASE II, unless there existed a mass cut of M_{ZAMS} for BH formation (M_{cut}). If SN Ib/c progenitors with a sufficiently high final mass could not produce an ordinary SN Ib/c, the SN Ic rate would significantly decrease with decreasing metallicity even with CASE II.

- For CASE II, SNe Ic with hydrogen or SNe IIc are expected to occur at sufficiently low metallicity (cf. Elmhamdi et al. 2006). Dessart et al. (2012a) indeed showed that SNe IIc can be produced if helium is effectively shielded from radioactive nickel.
- The SN Ib/SN IIb ratio would decrease with decreasing metallicity for both cases, which is in good agreement with the recent observation by Arcavi et al. (2010).
- Comparison of Figures 10 and 12 implies that both the initial and final masses of SNe Ic progenitors would be systematically higher than those of SN Ib progenitors, regardless of the adopted demarcation criterion of helium. This prediction is in qualitative agreement with SN observations (Cano 2013; Lyman et al. 2014; Taddia et al. 2014) and the stronger association of SNe Ic with younger stellar population than SNe Ib in the host galaxies (e.g., Anderson et al. 2012; Kelly & Kirshner 2012; Sanders et al. 2012).
- For CASE II, the average ejecta masses would increase following the order of SN Ib, IIb and Ic at sufficiently low metallicity.
- The average ejecta masses of SN Ib/c would increase with decreasing metallicity. This effect would be more dramatic for SNe Ic than for SNe Ib (see Figure 10).
- The comparison of Figures 10 and 12 indicates that for CASE II, the maximum final mass of SN Ib (and IIb) would be limited to a fairly small value (about $7.0 M_{\odot}$ with the assumed value of $M_{\text{He}}/M_{\text{ejecta}} = 0.45$) even for very low metallicity.

3.7. Surface properties and the progenitor candidate of iPTF13bvn

As explained in Section 3.2, a relatively low-mass helium star progenitor of SN Ib/c in binary systems undergo rapid expansion of its envelope during the carbon burning phase and later stages. This envelope expansion becomes stronger for a lower mass star for which the carbon-oxygen core becomes more compact, following the mirror effect (Yoon et al. 2010, 2012b; Eldridge et al. 2013). Within the framework discussed in Section 3.6, therefore, SNe Ib progenitors would have a more extended envelope than SN Ic progenitors for most cases, which may in turn lead a more luminous early plateau in the consequent SN (Dessart et al. 2011).

The extended envelope at the pre-SN stage can make an SN Ib/c progenitor fairly bright in the optical. The expected visual magnitude is about -4 to -5 for the progenitors having final masses of $3-5 M_{\odot}$ (Yoon et al. 2012b; Bersten et al. 2014; Eldridge et al. 2015; Kim, Yoon, & Koo 2015). With an O-type star companion, the visual brightness would be even higher ($M_V \simeq -6$ to -7). By contrast, WR star progenitors ($M_{\text{ZAMS}} \gtrsim 30 M_{\odot}$) from both single and binary stars have much higher bolometric luminosities, but the expected high surface temperatures at the pre-SN stage result in fainter visual brightness (i.e., $M_V \simeq -3$; Yoon et al. 2012b; Groh et al. 2013a) in most cases, which would make them more

difficult to directly identify in pre-SN images as discussed in Section 2.2.

Recently, Cao et al. (2013) have reported the tentative identification of the progenitor of the SN Ib iPTF13bvn. The estimated absolute magnitudes of the object in the optical range from -5.0 to -7 , depending on the filters, adopted extinction values, and photometry methods (Cao et al. 2013; Bersten et al. 2014; Eldridge et al. 2015). Groh, Georgy, & Ekstroem (2013b) argued for a single star progenitor with initial masses of $31-35 M_{\odot}$ based on the non-rotating models of the Geneva group. Unlike more massive stars that become WO stars at the end, these models end their lives as WN stars having relatively thick helium envelopes with surface temperatures of about $\log T_{\text{eff}} \sim 4.6$. The predicted optical magnitudes (~ -5.5) agree with the observation, but the final mass ($\sim 11 M_{\odot}$) seems to be too high, compared to the estimated ejecta mass of the SN ($\sim 1.9-2.3 M_{\odot}$; Fremling et al. 2014; Bersten et al. 2014) that supports the binary scenario. The optical brightness of the progenitor candidate can also be explained by a binary progenitor having an initial mass of $10-20 M_{\odot}$ (Bersten et al. 2014; Eldridge et al. 2015). If future observations find evidence for the companion star that survives the SN explosion, it will directly confirm a binary star origin of SNe Ib for the first time.

3.8. Rotation

Massive stars in a close binary system before mass transfer are likely to be synchronised with the orbit because of the short tidal interaction timescale. After Case B/AB mass transfer, the orbit becomes too wide to keep the tidal synchronisation, and the final rotation velocity of the primary star is mainly determined by the amount of angular momentum that is retained after the mass transfer phase. Binary evolution models including the effects of rotation indicate that SN Ib/c progenitors via Case B/AB mass transfers are slow rotators as they lose mass and angular momentum (Wellstein 2001; Yoon et al. 2010; Langer 2012). Both models with and without magnetic torques due to the Tayler–Spruit dynamo (see Section 2.4 for the discussion on angular momentum redistribution inside stars) predict that the surface rotation velocity of naked helium stars on the helium main sequence after the mass transfer phase is only about $1.0-10.0 \text{ km s}^{-1}$.

The specific angular momentum in the innermost region of $1.4 M_{\odot}$ that would collapse to a neutron star significantly according to the prescription of angular momentum transfer (Yoon et al. 2010). Models without the Tayler–Spruit dynamo predict that neutron stars from SNe Ib/c in binary systems would almost reach the critical rotation. This means that the majority of SN Ib/c progenitors in binary systems would also be good progenitor candidates for magnetars/collapsars without the Tayler–Spruit dynamo, which cannot be easily reconciled with observations. Models with the Tayler–Spruit dynamo predict that the specific angular momentum of the collapsing core would be comparable to

those of single star models (i.e., $j \sim 10^{14} \text{ cm s}^{-1}$) and the resultant neutron stars would be rotating at a period of several milliseconds.

As in the case of single stars, therefore, binary models with the Tayler–Spruit dynamo do not predict magnetar/collapsar progenitors for energetic SNe and/or long GRBs via the standard Case B/BB/AB/ABB systems (Yoon et al. 2010) under normal circumstances. At sufficiently low metallicity, however, mass accreting stars in Case B mass transfer systems may be spun up to undergo the chemically homogeneous evolution, which may end up as a GRB (Cantiello et al. 2007). SN Ib/c progenitors in very close binary systems consisting of a helium star and a low-mass main-sequence star/compact object (cf. Figure 6; Section 3.2) may experience strong tidal interaction, given that the orbital period can be as short as 0.1 d in this case (e.g., Dewi et al. 2002; Ivanova et al. 2003; Izzard et al. 2004; van den Heuvel & Yoon 2007; Detmers et al. 2008; Podsiadlowski et al. 2010). Some of these systems may produce unusually rapid rotators even within the framework of the Tayler–Spruit dynamo, but more detailed evolutionary studies are needed to make a meaningful conclusion on this. The fact that host galaxies of broad-lined SNe Ic and GRBs are found to be systematically overdense compared to other galaxies of the Sloan Digital Sky Survey might be an indication for the importance of the binary channel for producing rapidly rotating progenitors to produce these events (Kelly et al. 2014).

3.9. Observational counterparts

WR stars in binary systems are excellent observational counterparts for SN Ib/c progenitors during the post Case B/AB mass transfer phase, for $\log L/L_{\odot} \gtrsim 5.0$ (van der Hucht 2001). Relatively low-mass helium stars ($\log L/L_{\odot} < 5.0$) in binary systems are only rarely observed. This is probably because such helium stars on the helium main sequence are very hot and faint in optical bands (see Figure 8) and because many of them have bright OB-type companion stars.

As mentioned above (Section 3.3), the best observational counterpart of binary SN Ib/c progenitors with $\log L/L_{\odot} < 4.5$ is the qWR star HD 45166 (van Blerkom 1978; Willis & Stickland 1983; Steiner & Oliveira 2005; Groh, Oliveira, & Steiner 2008): the primary is a helium rich $4.2\text{-}M_{\odot}$ star with $R \simeq 1.0 R_{\odot}$ and the secondary is a $4.8\text{-}M_{\odot}$ main-sequence star, in a 1.596-d orbit (Steiner & Oliveira 2005). This system was probably produced via unstable Case B/AB mass transfer and the consequent common envelope phase. This star gives important information about the mass-loss rate from such a relatively low-mass helium star as discussed in Section 3.3. WR 7a is another qWR star (Schwartz et al. 1990; Pereira et al. 1998; Oliveira, Steiner, & Cieslinski 2003). No companion of this star has been found so far. Radial periodicity of 0.204 d has been reported, and if this is related to binarity, its companion should be a low-mass main-sequence star

($M \lesssim 1.0 M_{\odot}$) or a compact object. To our knowledge, no estimate of the wind mass-loss rate from this star has been reported yet.

There also exist candidates for evolved helium giant stars beyond core helium exhaustion. They include ν Sgr, KS Per and LSS 4300 (Dudley & Jeffery 1993). Among these, the ν Sgr system has been best studied (e.g., Frame et al. 1995; Saio 1995; Koubský et al. 2006; Netolický et al. 2009; Kipper & Klochkova 2012). The mass, surface temperature, and bolometric luminosity of the hydrogen-deficient primary of this system are $M \approx 3.0 M_{\odot}$, $T_{\text{eff}} \approx 11\,800 \text{ K}$ and $\log L/L_{\odot} \approx 4.6$. It also shows radial pulsation of a 20-d period (Saio 1995), and evidence for mass transfer and a circumbinary disk (Netolický et al. 2009), which agrees well with the Case BB mass transfer scenario (Schönberner & Drilling 1983). Therefore, these systems can provide useful information about the progenitor evolution as well as their circumstellar environments immediately before SN explosion. The visual magnitude of this star is $M_V = -4.73 \pm 0.3$ (Kipper & Klochkova 2012), which is consistent with the model predictions discussed in Section 3.7.

3.10. Companion stars

The companion stars of binary progenitors of SNe Ib/c will survive the SN explosion and may be found in some young SN remnants (e.g., Kochanek 2009; Koo et al. 2011). There may be several types of companion stars: main-sequence stars of early to late types, compact objects like white dwarfs, neutron stars and black holes, and helium stars (Section 3.1; Figure 6). In terms of stellar population, the most common type (i.e., more than 30% of all binary SN Ib/c progenitors) may be relatively high mass stars (O/B type) on the main sequence that underwent stable Case B/BB/AB/ABB mass transfer (e.g., Podsiadlowski et al. 1992; Eldridge et al. 2013). These massive companion stars accrete mass and angular momentum via stable mass transfer to be spun up to the critical value (Wellstein et al. 2001; Petrovic et al. 2005b; Cantiello et al. 2007; Yoon et al. 2010; Langer 2012; de Mink et al. 2013). At solar metallicity, however, they will lose angular momentum again via stellar winds after the mass transfer phase, and the rotation velocity shortly after the SN explosion depends on how much mass is lost by winds until that time. Models by Yoon et al. (2010) indicate that the surface rotation velocity will be about $300\text{--}450 \text{ km s}^{-1}$ for surviving companion of $M_2 \approx 17\text{--}20 M_{\odot}$. By contrast, more massive stars lose mass and angular momentum very quickly: a $48\text{-}M_{\odot}$ companion star would be slowed down to about 60 km s^{-1} at the pre-SN stage. The transferred mass to the secondary star is enriched with the ashes of hydrogen burning compared to the initial composition (de Mink et al. 2009; Langer 2012). The surface composition of the surviving secondary star after the SN explosion should be therefore marked by the enhancement of helium and nitrogen. The models of Yoon et al. (2010) give typically the mass fractions of helium and nitrogen of about 0.35 and 4.3×10^{-3} (i.e., 4.3 times

Table 1. Main predictions of single and binary star progenitors models for SNe Ib/c at solar metallicity.

	Single	Binary
Initial mass	$M_{\text{ZAMS}} \gtrsim 25 M_{\odot}$ at $Z = 0.02^a$	$M_{\text{ZAMS}} \gtrsim 12 M_{\odot}^b$
Final mass	$10 \lesssim M/M_{\odot} \lesssim 17$ at $Z = 0.02^a$	$1.4 < M/M_{\odot} \lesssim 17$ at $Z = 0.02^c$
Final radius	$0.5 \lesssim R/R_{\odot} \lesssim 10^d$	$0.5 \lesssim R/R_{\odot} \lesssim 100^e$
Wind mass-loss rate	$\dot{M} = 10^{-6} \sim 5 \times 10^{-5} M_{\odot} \text{yr}^{-1}$	$\dot{M} = 10^{-7} \sim 5 \times 10^{-5} M_{\odot} \text{yr}^{-1}$
Escape velocity ($\approx v_{\text{wind}}$)	$v_{\text{esc}} = 500\text{--}2500 \text{ km s}^{-1}$	$v_{\text{esc}} = 60\text{--}2500 \text{ km s}^{-1}$
Circumstellar structure	$\rho \propto r^{-2}$	Complex with wind–wind collision and orbital motion
Optical magnitudes	$M_{\text{V}} \approx -3$ for WO type progenitor, and $M_{\text{V}} = -5.5 \dots -6.5$ for WN type progenitor. ^f	$M_{\text{V}} \approx -3 \dots -6.0$ for most helium star progenitors. It will be more luminous in optical bands with a bright companion. ^g
Light curves	Relatively faint at early times. Broad light curves	Fairly luminous early time plateau for $13 \lesssim M_{\text{ZAMS}} \lesssim 25 M_{\odot}$
Spectra	No or weak helium lines for most cases, and hence biased towards the production of SNe Ic ^h .	Helium lines even without non-thermal processes during the early time plateau phase for $13 \lesssim M_{\text{ZAMS}} \lesssim 25 M_{\odot}$

^aMeynet & Maeder (2003).

^bWellstein & Langer (1999), Yoon et al. (2010) and Eldridge et al. (2013).

^cBased on the result presented in Figure 10 and Yoon et al. (2010) (in the figure, $f_w = 10$ roughly corresponds to $Z = 0.02$). See also Eldridge et al. (2011).

^dGroh et al. (2013a, 2013b).

^eYoon et al. (2010, 2012b) and Eldridge et al. (2013, 2015).

^fYoon et al. (2012b) and Groh et al. (2013a, 2013b).

^gYoon et al. (2012b), Bersten et al. (2014), Eldridge et al. (2015) and Kim et al. (2015).

^hDessart et al. (2011, 2012a).

the solar value) at the surface of surviving companion stars, respectively.

4 CONCLUSIONS

We summarise the main predictions of single and binary star models for ordinary SN Ib/c progenitors in Table 1.

Many of WR progenitors would end their lives as a WO type star that is relatively faint with optical filters ($M_{\text{V}} \approx -3$; Yoon et al. 2012b; Groh et al. 2013a). Binary systems with a sufficiently high initial mass of the primary star can produce WR progenitors of which the properties would be very similar to those of single WR stars, but the presence of the companion star would result in rather complex structures of the circumstellar medium and the SN remnant (Koo et al. 2011). Compared to the single star case, the detectability of WR progenitors can be significantly enhanced with a luminous early type companion.

However, given the preference for lower masses of the initial mass function, the majority of binary progenitors should have several unique properties that are very different from WR progenitors. Their final masses at the pre-SN stage are systematically lower ($M_{\text{f}} \simeq 1.4\text{--}6 M_{\odot}$ for $M_{\text{ZAMS}} \simeq 12\text{--}25 M_{\odot}$) than those of WR progenitors ($M_{\text{f}} > 10 M_{\odot}$). This agrees well with the recent ejecta mass estimates of ordinary SNe Ib/c ($M_{\text{ejecta}} = 1\text{--}6 M_{\odot}$; Drout et al. 2011; Cano 2013; Lyman et al. 2014; Taddia et al. 2014). The current binary model predictions are also consistent with the observational facts that the association of the SN locations in their host galaxies with young stellar populations becomes stronger following the order of SN II, SN Ib and SN Ic (Sections 3.3 and 3.6), which is usually interpreted

within the single star scenario in the literature (e.g., Anderson et al. 2012; Kelly & Kirshner 2012; Sanders et al. 2012).

Despite their relatively low masses, the detectability of binary progenitors in optical bands is not necessarily lower than single WR star progenitors. To the contrary, a significant fraction of binary progenitors should have very high visual luminosities because relatively low-mass helium stars can rapidly expand during the late evolutionary stages, and/or because many of them would have luminous companion stars (Yoon et al. 2012b; Eldridge et al. 2013, 2015).

The SN models by Dessart et al. (2011) indicate that early time light curves and spectra would have the critical information about the nature of SN Ib/c progenitors. In particular, the plateau phase due to helium recombination at early times and He I lines formed with thermal processes during this phase would be strong evidence for a relatively low-mass helium star progenitor having an extended helium envelope. As demonstrated by several recent observations (e.g., Soderberg et al. 2008; Modjaz et al. 2009; Corsi et al. 2012; Maeda et al. 2014), the progenitor size can also be best constrained by early-time SN light curves including shock breakouts. We therefore conclude that observations of early-time light curves and spectra will be an excellent probe into the nature of SN Ib/c progenitors.

There still exist many unsolved problems and related future topics that should be addressed.

- A caveat in the above conclusions is that the predictions summarised in Table 1 are mostly based on the models at solar metallicity. The final masses of single star progenitors at super-solar metallicity can become

as low as $5 M_{\odot}$, depending on the adopted mass-loss rate (Figure 2; Meynet & Maeder 2005). This value is within the ejecta mass range of ordinary SNe Ib/c by Cano (2013) and Lyman et al. (2014), although it still cannot explain SNe Ib/c having ejecta masses lower than about $3.5 M_{\odot}$. Given that the final amounts of helium must also be smaller than in the case of solar metallicity (Figure 11), the contribution from super-solar metallicity single stars might be particularly significant for SNe Ic (cf., Prieto, Stanek, & Beacom 2008; Boissier & Prantzos 2009; Modjaz et al. 2011).

- Although the SN Ib/c event rate implies the dominant role of binary systems for the production of SNe Ib/c (Smith et al. 2011; Eldridge et al. 2013), more direct evidence for binary progenitors comes from SNe Ib/c ejecta masses (M_{ejecta} ; Sections 3.3 and 3.6). Precise estimates of SN ejecta masses can give one of the best constraints for progenitor models. The uncertainties related to the effects of asymmetry of the explosion, mixing of chemical compositions in the SN ejecta and the presence of helium on the estimates of M_{ejecta} using SN light curves should be clarified in the near future (cf. Dessart et al. 2012a; Piro & Morozova 2014; Wheeler, Johnson, & Clocchiatti 2014).
- The question on how much helium can be hidden in SN Ic spectra is another critical test case for SN Ib/c progenitor models (Sections 2.3, 3.4 and 3.6; Figure 12). Recent observations indicate very low helium mass ($<0.14 M_{\odot}$) in the ejecta (Hachinger et al. 2012; Taddia et al. 2014). This cannot be easily accommodated to the current model predictions that most SN Ib/c progenitors have $M_{\text{He}} > 0.2$. This conflict may be due to our lack of proper knowledge on the mass-loss rate from helium stars (in particular during the post-helium burning phase; Section 3.4) but a rigorous estimate of helium masses for a large sample of SNe Ib/c is highly required to resolve this issue. The ratio of SN Ic to SN Ib is another important constraint for progenitor models, which should be better estimated in the future. Several authors reported that the Ic to Ib ratio is about 2 (e.g., Smartt 2009; Li et al. 2011), but Modjaz et al. (2014) point out that many SNe Ib had been misclassified as SNe Ic, suggesting a lower value.
- As discussed in Section 3.6, future observations on SN Ib/c and SN Iib properties and their relative frequencies as a function of metallicity (e.g., Prieto et al. 2008; Boissier & Prantzos 2009; Modjaz et al. 2011; Graham & Fruchter 2013) would greatly help to clarify the role of mass loss from helium stars in the evolution of SN Ib/c progenitors. It would be particularly important to investigate how the ejecta masses of SNe Ib/c and the ratio of SN Ib/SN Ic rate systematically depend on metallicity.
- In the discussions above, we did not address progenitors of broad-lined SNe Ic (SNe Ic-BL), simply because we do not have a good clue on what makes them. The

association of long GRBs and some SNe Ic-BL (e.g., Woosley & Heger 2006) implies the importance of rapid rotation, and attempts have been made to explain long GRBs, SNe Ic-BL and super-luminous SNe Ic within the single framework of the magnetar scenario (e.g., Mazzali et al. 2014). Binary star models including rotation do not predict any particular parameter space where unusually rapid rotation in the core can be realised from the standard Case B/BB/AB/ABB channels for SNe Ib/c (Petrovic et al. 2005b; Yoon et al. 2010), except for the so-called chemically homogeneous evolution induced by mass accretion at low metallicity (Cantiello et al. 2007). Future studies should investigate more carefully the evolution of some specific binary systems where the condition of rapid rotation for magnetars can be rather easily fulfilled compared to the standard channels, such as binary systems consisting of a helium star plus a compact object in a very tight orbit (Figure 6; Section 3.8).

ACKNOWLEDGEMENTS

The author is grateful to Norbert Langer, Stan Woosley, Luc Dessart, Hyun-Jeong Kim, Bon-Chul Koo, Götz Gräfener, Jorick Vink, Wonseok Chun, Thomas Tauris, Rob Izzard, Alexandra Kozyreva, and John Hillier for their contribution to this work and fruitful collaboration, and John Eldridge, Maryam Modjaz, Philipp Podsiadlowski, Ken'ichi Nomoto, Keiichi Maeda, Selma de Mink and Cyril Georgy for helpful discussions. This work was supported by Basic Science Research (2013R1A1A2061842) program through the National Research Foundation of Korea (NRF) and by Research Resettlement Fund for the new faculty of SNU.

References

- Anderson, J. P., Habergham, S. M., James, P. A., & Hamuy, M. 2012, MNRAS, 424, 1372
- Arcavi, I., et al. 2010, ApJ, 721, 777
- Barkat, Z., Rakavy, G., & Sack, N. 1967, PhRvL, 18, 379
- Bersten, M., et al. 2014, ApJ, 148, 68
- Boissier, S., & Prantzos, N. 2009, A&A, 503, 137
- Branch, D., et al. 2002, ApJ, 566, 1005
- Braun, H. 1997, PhD thesis, Ludwig-Maximilians University of Munich
- Burrows, A., Dessart, L., Livne, E., Ott, C. D., & Murphy, J. 2007, ApJ, 664, 416
- Cao, Y., et al. 2013, ApJ, 775, L7
- Cano, Z. 2013, MNRAS, 434, 1098
- Cano, Z., Maeda, K., & Schulze, S. 2014, MNRAS, 785, 95
- Cantiello, M., Mankovich, C., Bildsten, L., Christensen-Dalsgaard, J., & Paxton, B. 2014, ApJ, 788, 93
- Cantiello, M., Yoon, S.-C., Langer, N., & Livio, M. 2007, A&A, 465, 29
- Chevalier, R. A., & Soderberg, A. 2010, ApJ, 711, L40
- Chiosi, C., & Maeder, A. 1986, ARA&A, 24, 328
- Chomiuk, L., et al. 2011, ApJ, 743, 114
- Chornock, R., et al. 2011, ApJ, 739, 41

- Claeys, J. S. W., de Mink, S. E., Pols, O. R., Eldridge, J. J., & Baes, M. 2011, *A&A*, 528, A131
- Conti, P. S. 1976, In Proc. 20th Colloq. Int. Astrophys. Liège, p. 193, Univ. Liège
- Corsi, A., et al. 2012, *ApJ*, 747, 5
- Crockett, R. M., et al. 2007, *MNRAS*, 381, 835
- Crowther, P. A. 2007, *ARA&A*, 45, 177
- de Jager, C., Nieuwenhuijzen, H., & van der Hucht, K. A. 1988, *A&AS*, 72, 259
- de Mink, S. E., Langer, N., Izzard, R. G., Sana, H., & de Koter, A. 2013, *ApJ*, 764, 166
- de Mink, S. E., Pols, O. R., Langer, N., & Izzard, R. G. 2009, *A&A*, 507, 169
- de Mink, S. E., Sana, H., Langer, N., Izzard, R. G., & Schneider, F. R. N. 2014, *ApJ*, 782, 7
- Deng, J. S., Qiu, Y. L., Hu, J. Y., Hatano, K., & Branch, D. 2000, *ApJ*, 540, 452
- Dessart, L., Hillier, D. J., Livne, E., Yoon, S.-C., Woosley, S. E., Waldman, R., & Langer, N. 2011, *MNRAS*, 414, 2985
- Dessart, L., Hillier, D., Li, C., & Woosley, S. E. 2012a, *MNRAS*, 424, 2139
- Dessart, L., Hillier, D., Waldman, R., Livne, E., & Blondin, S. 2012b, *MNRAS*, 426, L76
- Detmers, R. G., Langer, N., Podsiadlowski, Ph., & Izzard, R. G. 2008, *A&A*, 484, 831
- Dewi, J. D. M., Pols, O. R., Savonije, G. J., & van den Heuvel, E. P. J. 2002, *MNRAS*, 331, 1027
- Drout, M. R., et al. 2011, *ApJ*, 741, 97
- Dudley, R. E., & Jeffery, C. S. 1993, *MNRAS*, 262, 945
- Eggenberger, P., Maeder, A., & Meynet, G. 2005, *A&A*, 440, L9
- Eggenberger, P., Montalbán, J., & Miglio, A. 2012, *A&A*, 544, L4
- Ekström, S., et al. 2012, *A&A*, 537, A146
- Eldridge, J. J., Fraser, M., Mound, J. R., & Smartt, S. J. 2015, *MNRAS*, 446, 2689
- Eldridge, J. J., Fraser, M., Smartt, S. J., Mound, J. R., & Crockett, R. M. 2013, *MNRAS*, 436, 774
- Eldridge, J. J., Izzard, R. G., & Tout, C. A. 2008, *MNRAS*, 384, 1109
- Eldridge, J. J., Langer, N., & Tout, C. A. 2011, *MNRAS*, 414, 3501
- Eldridge, J. J., & Vink, J. S. 2006, *A&A*, 452, 295
- Elmhamdi, A., Danziger, I. J., Branch, D., Leibundgut, B., Baron, E., & Kirchner, R. P. 2006, *A&A*, 450, 305
- Filippenko, A. V. 1997, *ARA&A*, 35, 309
- Foley, R. J., Smith, N., Ganeshalingam, M., Li, W., Chornock, R., & Filippenko, A. V. 2007, *ApJ*, 657, 105
- Frame, D. J., Cottrell, P. L., Gilmore, A. C., Kilmartin, P. M., & Lawson, W. A. 1995, *MNRAS*, 276, 383
- Fremming, C., et al. 2014, *A&A*, 565, 114
- Fryer, C. L., & Heger, A. 2005, *ApJ*, 623, 302
- Fujimoto, M. Y. 1993, *ApJ*, 419, 768
- Gal-Yam, A. 2009, *Nature*, 462, 624
- Gal-Yam, A., et al. 2014, *Nature*, 509, 471
- Gellert, M., Rüdiger, G., & Elstner, D. 2008, *A&A*, 479, L33
- Georgy, C., Ekström, S., Meynet, G., Massey, P., Levesque, E. M., Hirschi, R., Eggenberger, P., & Maeder, A. 2012, *A&A*, 542, A29
- Gorbikov, E., et al. 2014, *MNRAS*, 443, 671
- Gräfener, G., & Hamann, W.-R. 2008, *A&A*, 482, 945
- Gräfener, G., Owocki, S. P., & Vink, J. S. 2012, *A&A*, 538, A40
- Gräfener, G., & Vink, J. S. 2013, *A&A*, 560, A6
- Graham, J. F., & Fruchter, A. S. 2013, *ApJ*, 774, 119
- Groh, J. H., Oliveira, A. S., & Steiner, J. E. 2008, *A&A*, 485, 245
- Groh, J. H., Meynet, G., Georgy, C., & Ekstroem, S. 2013a, *A&A*, 558, A131
- Groh, J. H., Georgy, C., & Ekstroem, S. 2013b, *A&A*, 558, L1
- Hachinger, S., Mazzali, P. A., Taubenberger, S., Hillebrandt, W., Nomoto, K., & Sauer, D. N. 2012, *MNRAS*, 422, 70
- Hakobyan, A. A., Mamon, G. A., Petrosian, A. R., Kunth, D., & Turatto, M. 2009, *A&A*, 508, 1259
- Hamann, W.-R., Gräfener, G., & Liermann, A. 2006, *A&A*, 457, 1015
- Hamann, W.-R., Koesterke, L., & Wessolowski, U. 1995, *A&A*, 299, 151
- Hamann, W.-R., Schoenberner, D., & Heber, U. 1982, *A&A*, 116, 273
- Heger, A., Fryer, C. L., Woosley, S. E., Langer, N., & Hartmann, D. H. 2004, *ApJ*, 591, 288
- Heger, A., Langer, N., & Woosley, S. E. 2000, *ApJ*, 528, 368
- Heger, A., Woosley, S. E., & Spruit, H. C. 2005, *ApJ*, 626, 350
- Hirschi, R., Meynet, G., & Maeder, A. 2004, *A&A*, 425, 649
- Hjorth, J. 2013, *PTRSL*, 371, 20120275
- Ibeling, D., & Heger, A. 2013, *ApJ*, 765, 43
- Inserra, C., et al. 2013, *ApJ*, 770, 128
- Ishii, M., Ueno, M., & Kato, M. 1999, *PASJ*, 51, 417
- Ivanova, N., Belczynski, K., Kalogera, V., Rasio, F. A., & Taam, R. E. 2003, *ApJ*, 592, 475
- Izzard, R. G., Ramirez-Ruiz, E., & Tout, C. A. 2004, *MNRAS*, 348, 1215
- Jeffery, C. S., & Hamann, W.-R. 2010, *MNRAS*, 404, 1698
- Justham, S., Podsiadlowski, Ph., & Vink, J. S. 2014, *ApJ*, 796, 121
- Kasen, D., & Bildsten, L. 2010, *ApJ*, 717, 245
- Kelly, P. L., Filippenko, A. V., Modjaz, M., & Kocevski, D. 2014, *ApJ*, 789, 23
- Kelly, P. L., & Kirshner, R. P. 2012, *ApJ*, 759, 107
- Kim, H.-J., Yoon, S.-C., & Koo, B.-C. 2015, *ApJ*, submitted
- Kippenhahn, R., & Weigert, A. 1967, *ZA*, 65, 251
- Kipper, T., & Klochkova, V. G. 2012, *BaltA*, 21, 219
- Kobulnicky, H. A., & Fryer, C. L. 2007, *ApJ*, 670, 747
- Kochanek, C. 2009, *ApJ*, 707, 1578
- Koo, B. C., et al. 2011, *ApJ*, 732, 6
- Koubsk'y, P., Harmanec, P., Yang, S., Netolický, M., Netolick, M., Škoda, P., Šlechta, M., & Korčáková, D. 2006, *A&A*, 459, 849
- Kozyreva, A., Blinnikov, S., Langer, N., & Yoon, S.-C. 2014, *A&A*, 565, 70
- Langer, N. 1989a, *A&A*, 210, 93
- Langer, N. 1989b, *A&A*, 220, 135
- Langer, N. 1992, *A&A*, 265, 17
- Langer, N. 2012, *ARA&A*, 50, 107
- Lauterborn, D. 1970, *A&A*, 7, 150
- Li, W., et al. 2011, *MNRAS*, 412, 1441
- Lucy, L. B. 1991, *ApJ*, 383, 308
- Lunnan, R., et al. 2014, *ApJ*, 787, 138
- Lyman, J., et al. 2014, arXiv:1406.3667
- MacFadyen, A., & Woosley, S. 1999, *ApJ*, 524, 262
- Maeda, K., Katsuda, S., Bamba, A., Terada, Y., & Fukazawa, Y. 2014, *ApJ*, 785, 95
- Maeder, A. 1987, *A&A*, 178, 159
- Maeder, A., & Meynet, G. 1987, *A&A*, 182, 243
- Maeder, A., & Meynet, G. 2000, *ARA&A*, 38, 143

- Maeder, A., Georgy, C., Meynet, G., & Ekström, S. 2012, *A&A*, 539, A110
- Massey, Ph. 2003, *ARA&A*, 41, 15
- Maund, J. R., & Smartt, S. J. 2005, *MNRAS*, 360, 288
- Maund, J. R., Smartt, S. J., Kudritzki, R. P., Podsiadlowski, Ph., & Gilmore, G. F. 2004, *Nature*, 427, 129
- Maund, J. R., Smartt, S. J., & Schweizer, F. 2005, *ApJ*, 630, 33
- Mazzali, P. A., McFadyen, A. I., Woosley, S. E., Pian, E., & Tanaka, M. 2014, *MNRAS*, 443, 67
- Mazzali, P. A., Röpke, F. K., Benetti, S., & Hillebrandt, W. 2007, *Science*, 315, 825
- Meynet, G., & Maeder, A. 1997, *A&A*, 321, 465
- Meynet, G., & Maeder, A. 2003, *A&A*, 404, 975
- Meynet, G., & Maeder, A. 2005, *A&A*, 429, 581
- Meynet, G., Maeder, A., Schaller, G., Schaerer, D., & Charbonnel, C. 1994, *A&AS*, 103, 97
- Modjaz, M., et al. 2014, *ApJ*, 147, 99
- Modjaz, M., Kewley, L., Bloom, J. S., Filippenko, A. V., Perley, D., & Silverman, J. M. 2011, *ApJ*, 731, 4
- Modjaz, M., et al. 2008, *AJ*, 135, 1136
- Modjaz, M., et al. 2009, *ApJ*, 702, 226
- Netolický, M., Bonneau, D., Cehsneau, O., Harmanec, P., Koubsk, P., Mourard, D., & Stee, P. 2009, *A&A*, 499, 827
- Nicholl, M., et al. 2013, *Nature*, 502, 346
- Nomoto, K., Yamaoka, H., Pols, O. R., van den Heuvel, E. P. J., Iwamoto, k., Kumagai, S., & Shigeyama, T. 1994, *Nature*, 371, 227
- Nugis, T., & Lamers, H. J. G. L. M. 2000, *A&A*, 360, 227
- Oliveira, A. S., Steiner, J. E., & Cieslinski, D. 2003, *MNRAS*, 346, 963
- Pereira, C. B., Machado, M. A. D., Landaberry, S. J. C., & da Conceicao, F. 1998, *A&A*, 338, L91
- Petrovic, J., Langer, N., & van der Hucht, K. A. 2005a, 435, 1013
- Petrovic, J., Langer, N., Yoon, S.-C., & Hger, A. 2005b, 435, 247
- Petrovic, J., Pols, O., & Langer, N. 2006, *A&A*, 450, 219
- Piro, A., & Morozova, V. S. 2014, *ApJ*, 792, L11
- Podsiadlowski, Ph., Hsu, J. J. L., Joss, P. C., & Ross, R. R. 1993, *Nature*, 364, 509
- Podsiadlowski, Ph., Ivanova, N., Justham, S., & Rappaport, S. 2010, *MNRAS*, 406, 840
- Podsiadlowski, Ph., Joss, P. C., & Hsu, J. J. L. 1992, *ApJ*, 391, 246
- Pols, O. R. 1994, *A&A*, 290, 119
- Pols, O. R., & Dewi, J. D. M. 2002, *PASA*, 19, 233
- Prieto, J. L., Stanek, K. Z., & Beacom, J. F. 2008, *ApJ*, 673, 999
- Saio, H. 1995, *MNRAS*, 277, 1393
- Salasnich, B., Bressan, A., & Chiosi, C. 1999, *A&A*, 342, 131
- Sana, H., et al. 2012, *Science*, 337, 444
- Sander, A., Hamann, W.-R., & Todt, H. 2012, *A&A*, 540, A144
- Sanders, N. E., et al. 2012, *ApJ*, 758, 132
- Scalzo, R. A., Ruitter, A. J., & Sim, S. A. 2014, *MNRAS*, 445, 2535
- Schaeffer, R., Casse, M., & Cahen, S. 1987, *ApJ*, 316, L31
- Schaerer, D., Charbonnel, C., Meynet, G., Maeder, A., & Schaller, G. 1993a, *A&AS*, 102, 339
- Schaerer, D., Meynet, G., Maeder, A., & Schaller, G. 1993b, *A&AS*, 98, 523
- Schaller, G., Schaerer, D., Meynet, G., & Maeder, A. 1992, *A&AS*, 96, 269
- Schoenberner, D., & Drilling, J. S. 1983, *ApJ*, 268, 225
- Schwartz, R. D., Persson, S. E., & Hamann, F. W. 1990, *AJ*, 100, 793
- Smartt, S. J. 2009, *ARA&A*, 47, 63
- Smith, N. 2014, *ARA&A*, 53, 487
- Smith, N., Li, W., Filippenko, A. V., & Chornock, R. 2011, *MNRAS*, 412, 1522
- Soderberg, A. M., et al. 2008, *Nature*, 453, 469
- Spencer, J., & Baron, E. 2010, *ApJ*, 718, 957
- Spruit, H. C. 2002, *A&A*, 381, 923
- Steiner, J. E., & Oliveira, A. S. 2005, *A&A*, 444, 895
- Stritzinger, M., Leibundgut, B., Walch, S., & Contardo, G. 2006, *A&A*, 450, 241
- Suijs, M. P. L., Langer, N., Poelarends, A.-J., Yoon, S.-C., Heger, A., & Herwig, F. 2008, *A&A*, 481, 87
- Taddia, F., et al. 2014, *A&A*, 574, A60
- Tauris, T. M., Langer, N., Moriya, T. J., Podsiadlowski, Ph., Yoon, S.-C., Blinnikov, S. I. 2013, *ApJ*, 778, L23
- Townsend, R., & MacDonald, J. 2008, in *IAU Symp. Vol. 250, Massive stars as cosmic engines*, eds. F. Bresolin, P. A. Crowther & J. Puls (Cambridge: Cambridge University Press), 161
- Vanbeveren, D., De Loore, C., & Van Rensbergern, W. 1998, *A&AR*, 9, 63
- Vanbeveren, D., Van Bever, J., & Belkus, H. 2007, *ApJ*, 662, 107
- van Blerkom, D. 1978, *ApJ*, 225, 175
- van den Berg, S., Li, W., & Filippenko, A. V. 2005, *PASP*, 117, 773
- van den Heuvel, E. P. J., & Yoon, S.-C. 2007, *Ap&SS*, 311, 177
- van der Hucht, K. A. 2001, *NewAR*, 45, 135
- Van Dyk, S. D., et al. 2014, *ApJ*, 147, 37
- van Loon, J. Th., Cioni, M.-R. L., Zijlstra, A. A. & Loup, C. 2005, *A&A*, 438, 273
- van Loon, J. Th., et al. 2008, *A&A*, 487, 1055
- Vink, J. S., & de Koter, A. 2005, *A&A*, 442, 587
- Wellons, S., Soderberg, A. M., & Chevalier, R. A. 2012, *ApJ*, 752, 17
- Wellstein, S. 2001, PhD Thesis, University of Potsdam
- Wellstein, S., & Langer, N. 1999, *A&A*, 350, 148
- Wellstein, S., Langer, N., & Braun, H. 2001, *A&A*, 369, 939
- Wheeler, J. C., Johnson, V., & Clocchiatti, A. 2014, *arXiv:1411.5975*
- Wheeler, J. C., Yi, I., Höflich, P., & Wang, L. 2000, *ApJ*, 537, 810
- Willis, A. J., & Stickland, D. J. 1983, *MNRAS*, 203, 619
- Woosley, S. E. 1993, *ApJ*, 405, 273
- Woosley, S. E. 2010, *ApJ*, 719, 204
- Woosley, S. E., & Bloom, J. S. 2006, *ARA&A*, 44, 507
- Woosley, S. E., & Eastman, R. G. 1997, in *Thermonuclear Supernovae*, NATO ASI Proc. Sereis C., Vol. 486, ed. P. Ruiz-Lapuente, R. Canal, & J. Isern (Dordrecht: Kluwer), 821
- Woosley, S. E., & Heger, A. 2006, *ApJ*, 637, 914
- Woosley, S. E., Langer, N., & Weaver, T. A. 1993, *ApJ*, 411, 823
- Woosley, S. E., Langer, N., & Weaver, T. A. 1995, *ApJ*, 448, 315
- Yoon, S.-C., & Langer, N. 2005, *A&A*, 443, 643
- Yoon, S.-C., & Cantiello, M. 2010, *ApJ*, 717, L62
- Yoon, S.-C., Dierks, A., & Langer, N. 2012a, *A&A*, 542, A113
- Yoon, S.-C., Gräfener, G., Vink, J. S., Kozyreva, A., & Izzard, R. G. 2012b, *A&A*, 544, L11
- Yoon, S.-C., Langer, N., & Norman, C. 2006, *A&A*, 460, 199
- Yoon, S.-C., Woosley, S. E., & Langer, N. 2010, *ApJ*, 725, 940
- Zahn, J.-P., Brun, A. S., & Mathis, S. 2007, *A&A*, 474, 145